Assessing Macroeconomic Tail Risk

Francesca Loria* Christian Matthes† Donghai Zhang‡

April 21, 2024

Abstract

Real GDP and industrial production in the US display substantial asymmetry and tail risk. Is this asymmetry driven by a specific structural shock? Our empirical approach, based on quantile regressions and local projections, suggests otherwise. We find that the 10th percentile of predictive growth distributions responds between three and six times more than the median to monetary policy shocks, financial shocks, uncertainty shocks, and oil price shocks, indicating a common transmission mechanism. We present two data-generating processes that are capable of matching this finding: A threshold VAR model and a nonlinear equilibrium model.

Keywords: Macroeconomic Risk, Shocks, Local Projections

JEL Classification: C21, C53, E30, E37

We thank Marvin Nöller and Federico Alexander Rizzuto for excellent research assistance. We also want to thank Franck Portier, four anonymous referees, Danilo Cascaldi-Garcia, Dario Caldara, Fabio Canova, Todd Clark, Giovanni Favara, Domenico Giannone, Nobuhiro Kiyotaki, Ricardo Reis, Erick Sager, Rosen Valchev, and Alexander Wolman, as well as seminar/workshop participants at the Chinese University of Hong Kong, University of Bonn, International Finance Workshop on Quantile Regressions at the Board of Governors, 2019 IAAE conference, 2020 SNDE conference, "Modeling The Macroeconomy in Risky Times" Workshop in St. Louis, "Macro-at-Risk" session of the ECB Working Group on Econometric Modelling, IMF's "Monetary and Capital Markets (MCM) Policy Forum", SEACEN, and the Central Bank of Ireland for helpful comments.

Disclaimer: The views presented herein are those of the author and do not necessarily reflect those of the Federal Reserve Board, the Federal Reserve System or their staff.

*Board of Governors of the Federal Reserve System, francesca.loria@frb.gov.

†Indiana University, matthesc@iu.edu.

‡National University of Singapore, donghai.d.zhang@gmail.com.

1 Introduction

Recent contributions in macroeconomics and finance (Adrian, Boyarchenko and Giannone, 2019; Giglio, Kelly and Pruitt, 2016) have highlighted that growth in measures of US output is highly asymmetric and features substantial *tail risk*. To illustrate this feature, Figure 1 plots the quantiles of the one-year ahead forecast distribution of growth in Real Gross Domestic Product (GDP) and Industrial Production (IP), commonly called "growth-at-risk". We present the findings from Adrian, Boyarchenko and Giannone (2019) based on quarterly GDP, and also show that the findings are very similar when using the growth rate of industrial production instead, which is available at a monthly frequency and that we will rely on in our benchmark analysis.[1]

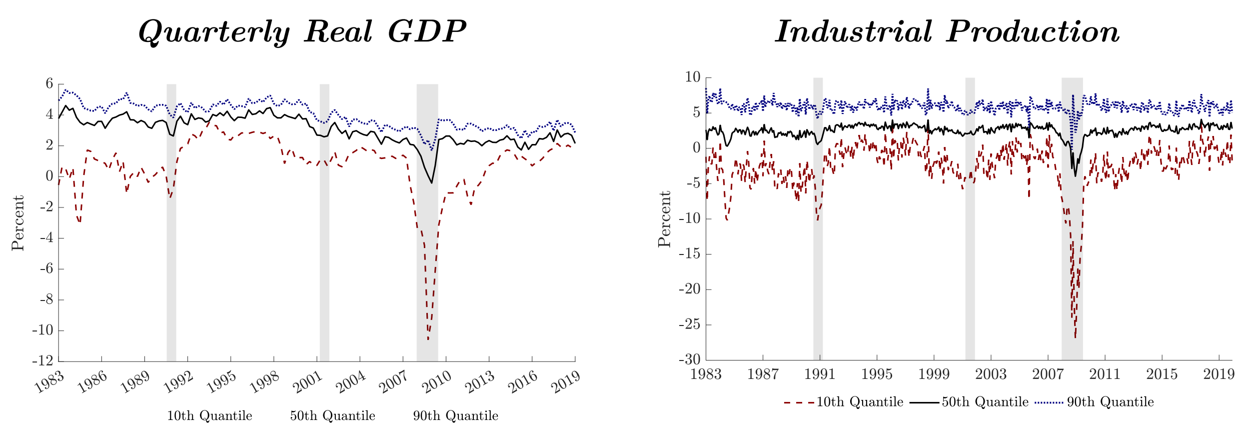

Figure 1: Quantiles of One-Year-Ahead Growth for Various Measures.

Note: Quantiles of Average Growth over the Next Year of quarterly Real GDP Growth from 1983-Q1 to 2019-Q4 and monthly Industrial Production Growth from January 1983 to December 2019. Grey-shaded bars indicate NBER-dated recessions.

Both panels convey the same asymmetry – the 10th quantile moves substantially more, in a recession, relative to the median or the 90th percentile.[2] While this fact is well documented, it is not clear what the source behind this asymmetry is. *Is this fact driven by a specific structural shock or is there a common transmission mechanism that leads to this asymmetry?*

[1] Giglio, Kelly and Pruitt (2016) focus on asymmetries in industrial production growth due to systemic risk.
[2] Details on the construction can be found in Section 3.1.

Previous empirical studies with a focus on nonlinearities have usually focused on one specific shock (e.g. Primiceri, 2005; Tenreyro and Thwaites, 2016; Hamilton, 2011; Barnichon *et al.*, 2022; Forni *et al.*, 2022). To answer the question we raised above we instead consider a battery of shocks in a common framework and proceed in two stages.

In the first stage, we use a convenient two-step estimation routine that merges ideas from Quantile Regression (Koenker and Bassett, 1978) to determine quantiles of the distribution of interest with Local Projections (Jordà, 2005) to assess the effects of monetary policy shocks, shocks to financial conditions, uncertainty shocks, and oil price shocks on the (predictive) distribution of the growth rate of Industrial Production (IP).[3] We devise a bootstrap algorithm to capture all relevant statistical uncertainty in this approach and that might be of independent interest to some readers. We find that responses to *all* shocks considered here show substantial asymmetry - over the first year the 10th percentile moves at least 3.5 times more than the median in response to the structural shocks.

In the second stage, we give two examples of data-generating processes (DGPs) that can create nonlinearities similar to those we find in US data.[4] We also use those DGPs as laboratories to test our empirical machinery. The first DGP, a "semi-structural" threshold model, makes transparent that a threshold VAR characterized by state-dependent elasticities and/or variances is sufficient to generate the nonlinearities we observe. The second DGP, the nonlinear DSGE model with financial panics by Gertler, Kiyotaki and Prestipino (2019), confirms that a common propagation mechanism amplifies downturns, thus supporting the plausibility of our empirical findings.

Our analysis is motivated by concerns that economic policymakers and market participants have long harbored: They are generally not only concerned about what changes in economic

[3] We focus on Industrial Production because it is available at monthly frequency. In an earlier version of this paper, we instead used a monthly measure of real GDP growth and found qualitatively very similar results.

[4] Clearly, those example are non-exhaustive: Many other data-generating processes are consistent with our findings. Our empirical framework is general enough to capture asymmetries independently of what exact DGP generated the data.

conditions will do to the economy *on average*, but also how these changes affect both the probability of *large* harmful events occurring as well as the magnitude of these events.[5] We borrow the concept of *value-at-risk* from the finance literature to operationalize the concept of macroeconomic tail risk. To be more precise, we follow Adrian, Boyarchenko and Giannone (2019) and study the distribution of macroeconomic risk by estimating a quantile forecast regression of real GDP growth over the next year for various quantiles.

Standard impulse response functions in linear models such as Vector Autoregressions (VARs) are not built to answer these questions, as they track average outcomes. While fully parametric VARs that specify the probability distribution of the one-step ahead forecast error could be used to derive such measures of risk, these VARs put many restrictions on the behavior of forecast densities.[6] Our goal is to provide a flexible, yet simple framework that can directly address these issues. A flexible approach is useful when studying GDP growth because GDP growth is far from Gaussian, as can be seen from papers that interpret the non-normality in GDP growth as coming from fat tails and/or stochastic volatility (Fagiolo, Napoletano and Roventini, 2008, Cúrdia, Del Negro and Greenwald, 2014, and Justiniano and Primiceri, 2008). Our approach is constructed to be flexible through the following modeling choices: In the initial quantile regression stage, we model each quantile separately instead of assuming a specific distribution for the forecast distribution of real GDP growth. In the second stage, we use local projections to impose as few restrictions on the data generating process as possible.[7] By predicting each quantile using both financial conditions and lagged IP growth, our approach can also shed light on whether any nonlinearities are transmitted via either of

[5]For research emphasizing that the Federal Reserve is concerned by downside risk, see Kilian and Manganelli (2008). For direct evidence of a policymaker thinking about downside risk (which we will use synonymously with tail risk), see March 2019 speech by Lael Brainard.

[6]Even non-linear time series models such as VARs with stochastic volatility and time-varying parameters along the lines of Cogley and Sargent (2005) and Primiceri (2005) impose substantial structure. Carriero, Clark and Marcellino (2020) propose an extension to the standard stochastic volatility structure embedded in these models that helps to capture tail risks.

[7]As shown by Plagborg-Møller and Wolf (2021), local projections and VARs asymptotically estimate the same impulse responses, but are on diametrically opposite ends of the bias-variance trade-off in finite samples.

those predictors or both jointly, as we highlight in Section 4.2.

While the main focus of our paper is on the empirical relationship between various structural shocks and the distribution of real activity, our paper also provides key insights on how to replicate growth-at-risk patterns in theoretical models via our two examples of classes of DGPs that can generate such findings. So far, there have been limited efforts in trying to rationalize results from the growth-at-risk literature and to use them as guidance for economic modeling. One such effort is Adrian, Liang, Zabczyk and Duarte (2020) which adapt a standard New Keynesian model to include "financial vulnerability" driven by movements in endogenous and forward looking financial conditions and calibrate it to match growth-at-risk patterns. Another example is Aikman, Bluwstein and Karmakar (2021) which build a semi-structural New Keynesian model with financial frictions and obtain a fat-tailed distribution of GDP. What distinguishes our approach is that we specifically build data-generating processes that explain our empirical evidence on the asymmetric effects of shocks on the growth outlook, as outlined above.

Our paper provides valuable insights for both policymakers and economists. We find that adverse shocks disproportionately increase the risk of downturns, highlighting the importance of nonlinearities in understanding the effects of standard shocks in equilibrium models for business cycle analysis. Additionally, we offer new stylized facts that can serve as calibration targets for macroeconomists building these equilibrium models.

The paper is organized as follows. Section 2 provides examples of impulse responses for quantiles to help with interpretation of our empirical results. Section 3 gives an overview of our methodology to estimate quantiles and their impulse responses to structural shocks. We then introduce the specifications and data transformations used in our empirical analysis in Section 4, which also presents our main results. In Section 5 we present a conceptual framework to rationalize and shed light on the potential mechanisms behind our findings. We offer concluding remarks and suggest avenues for future research in Section 6.

2 Intuition for Impulse Responses of Quantiles

This section gives three examples in which an initial distribution of a variable changes after a shock occurs. We show these examples to illustrate how a change in quantiles is linked to changes in the distribution as a whole and how changes in specific moments translate into changes in quantiles.[8] Our scenario is as follows: After an initial distribution of a scalar variable is hit by a shock, we trace out how this distribution changes on impact and in the period after impact. We consider three experiments:[9]

1. The shock leads to an increase in the variance of our distribution.

2. The shock leads to an increase in the mean of our distribution.

3. The shock leads to a change in *both* the mean and variance of our distribution.

Figure 2 plots three panels for each experiment. The first panel in each row shows the initial distribution, the distribution when the shock hits, and the distribution in the period after the shock has materialized. The middle panel in each row shows the evolution of the 10th and 90th percentile for those three periods. The last panel in each row gives the impulse responses for the 10th and 90th percentiles *under the assumption that if the shock that moved the distributions had not materialized, the distribution would have remained at its original position.*[10] As the impulse response plots the difference between the relevant percentiles and the original values, the impulse response figures only show values for two time periods (the period when the shock hits and the period after). Each row presents the figures for one experiment. Note that the levels of the percentiles are not directly interpretable as IRFs because we do not

[8] These examples are not meant to be exhaustive. There can be many other changes in distributions that lead to movements in quantiles similar to those displayed in this section.

[9] For simplicity all densities in this example are Gaussian. Our empirical approach makes no distributional assumptions.

[10] For our purposes, impulse responses are defined as the difference between two conditional expectations, where one of the expectations conditions on a specific value for one shock in one specific period.

subtract the baseline value from the quantiles in those figures. As we can see, an increase in the variance of a symmetric distribution makes the quantiles drift apart in a mirror-image fashion, whereas a change in the mean of a symmetric distribution makes the quantiles move in parallel, which in turn makes the impulse responses lie on top of each other. With a non-symmetric distribution (or if a shock makes a distribution non-symmetric) the quantiles can drift apart, but not necessarily in a mirror-image fashion, as highlighted in the third example.

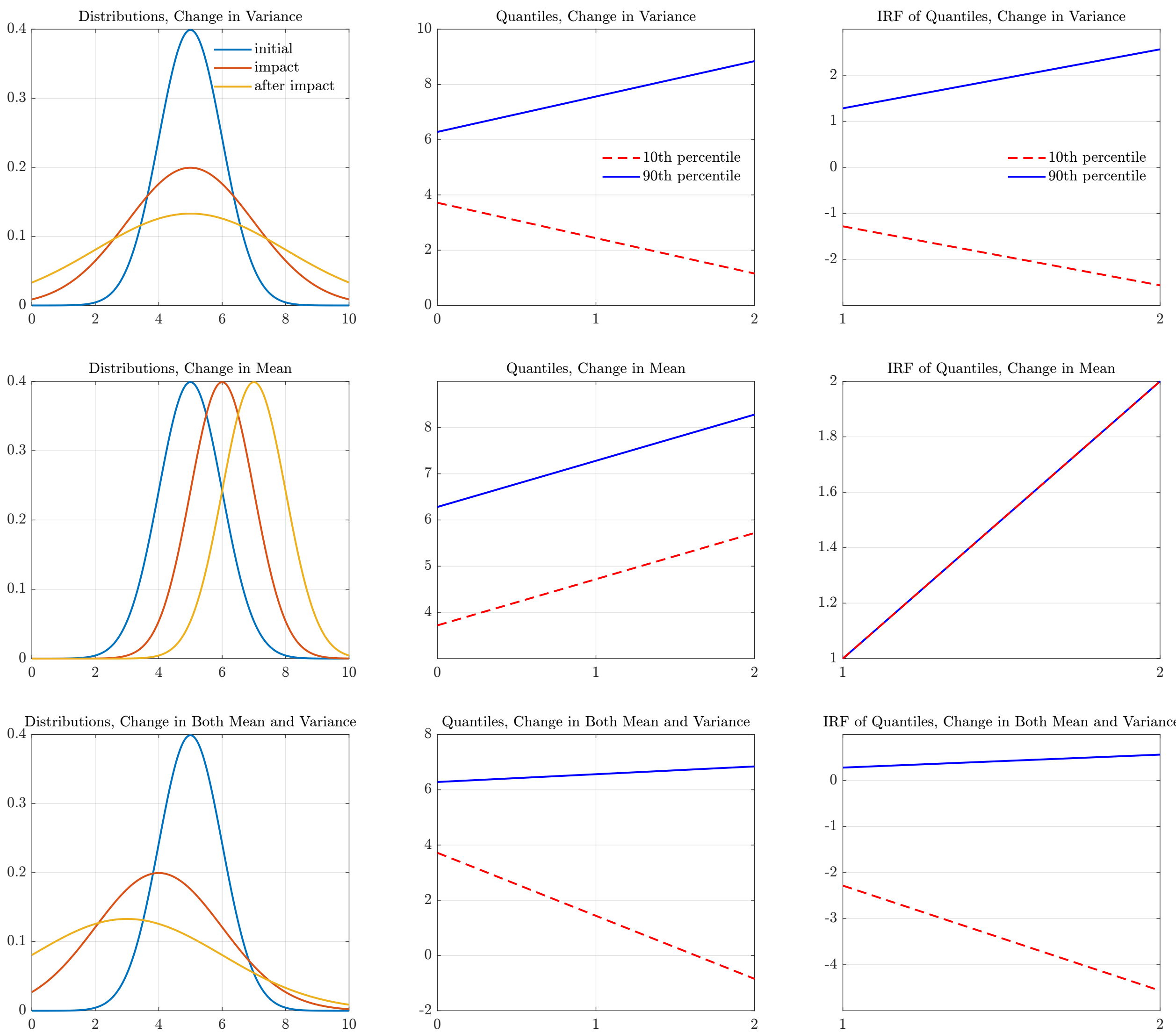

Figure 2: Illustration of Changes in Percentiles.

Interpreting changes in multiple quantiles jointly can be challenging because we have to envision how the entire distribution changes. As an example, let us focus on the third experiment. As can be seen in the last panel on the bottom row of Figure 2, the 10th and 90th percentile drift apart because the 90th percentile increases slightly, while the 10th percentile decreases substantially. Thus, the distribution *spreads out* as a result of the shock—this can also be seen by looking at the leftmost panel of the bottom row, where the yellow distribution is more spread out than the original blue distribution. Let us for a second imagine that this impulse response is the response to a contractionary shock and that quantiles react linearly to those shocks (as will be the case in our local projections). Such shocks would not only move the mean and median of the distribution (this can be seen from looking directly at the Gaussian distributions in the bottom left panel, where the mean/median of the Gaussian distribution moves from 5 to 3), but it actually moves the 10th percentile substantially more, thus not only making average outcomes worse, but making outcomes in the left tail much more likely. This is the relevant case in our empirical results.

Another scenario that could occur is that the impulse responses of various quantiles cross. It is important to emphasize that this does *not* mean that the quantiles themselves cross. In fact, a crossing of impulse responses of various quantiles can just mean that one quantile reverts back to its pre-shock value faster than another. We discuss this in more detail in Appendix A.

Our responses capture the difference between the expected path of the τth quantile at horizon h after a given shock of specific (one standard deviation) size occurs and the expected path of the τth quantile conditioning on such a specific shock value. That is, a response equal to 0 at horizon h means that the expected τth quantile at horizon h is the same independently of whether we condition on a specific shock value in the initial period.

3 Econometric Methodology

Our approach consists of two steps, which we outline in this section. First, we compute quantiles of the predictive distribution of one-year-ahead IP growth. We focus on the 10th percentile and, as reference points, the median and 90th percentile. We interpret this 10th percentile of the predictive distribution of future IP growth as *macroeconomic risk*. Our second step then uses local projections to assess how structural shocks affect macroeconomic risk and the predictive distribution of average future IP growth more generally.

3.1 Conditional Quantiles

Quantile regression models (Koenker and Bassett, 1978) are a flexible tool to quantify risks surrounding the growth outlook and to study its determinants.[11] The first step in our analysis is to use this methodology to compute conditional quantiles of future IP growth as in the quantile regression application in Adrian, Boyarchenko and Giannone (2019), with the important difference of moving to monthly frequency to allow a timely assessment of developments in financial markets and the real economy. The data are illustrated in Appendix B. Let us denote by ΔIP_t the annualized (real) industrial production growth rate, by $\bar{\Delta} IP_{t+1,t+12}$ its average over the next 12 months, and by $NFCI_t$ the Chicago Fed's National Financial Conditions Index. Formally, the conditional future IP growth quantiles are estimated from a linear quantile regression (QR) model whose predicted value

$$q_{\tau,t} \equiv \widehat{Q}_\tau(\bar{\Delta} IP_{t+1,t+12} | NFCI_t, \Delta IP_t) = \hat{\alpha}_\tau + \hat{\beta}_\tau NFCI_t + \hat{\gamma}_\tau \Delta IP_t, \quad \tau \in (0,1) \tag{3.1}$$

is a consistent estimator of the quantile function of $\bar{\Delta} IP_{t+1,t+12}$ conditional on the variables

[11] For an introduction to the quantile regression methodology, see Koenker (2005).

$\{\Delta IP_t, NFCI_t\}$.[12,13] For the estimation of the parameters, we use data from January 1983 to December 2019 (except for our monetary policy shock application, where we use data from February 1990 to December 2019 to align the QR sample with the sample available for our proxy). The estimated QR coefficients are reported in Appendix C.

The time evolution of the one-year-ahead predictive IP growth distribution can be illustrated through the fitted values for the 10th quantile (left tail), the median, and the 90th quantile (right tail). As previously shown in Figure 1, these quantiles (right panel) are similar to those obtained by Adrian, Boyarchenko and Giannone (2019) (left panel) at quarterly frequency (originally run for the period from 1973:Q1 to 2015:Q4, conditioning on NFCI and GDP growth).

3.2 Impulse Responses

Since the fitted quantiles summarize not only the median but, most importantly, the tails of the future IP growth distribution, they constitute a measure of macroeconomic (downside and upside) risk. Our interest lies in investigating whether and how these measures of risk respond to aggregate shocks. We estimate the responses of different future IP growth quantiles to a variety of aggregate shocks by applying the local projection method of Jordà (2005). As a baseline, we run the following linear regression:

$$q_{\tau,t+s} = \delta^s_\tau + \theta^s_\tau \ shock_t + \Psi(L)^s_\tau \ controls_t + u^s_{\tau,t+s}, \quad s = \{0,\ldots,S\} \tag{3.2}$$

where $q_{\tau,t+s}$ is the τth quantile computed in the previous section, $shock_t$ is the structural shock of interest, and $\Psi(L)^s_\tau \ controls_t$ is a lag polynomial of control variables which include

[12] Formally, the dependence between explanatory variables x_t and a quantile of y_t is measured by the coefficient $\hat{\beta}_\tau = \operatorname{argmin}_{\beta_\tau \in \mathbb{R}} \sum_{t=1}^{T} \left(\tau \cdot \mathbb{1}_{(y_t \geq x_t\beta)}|y_t - x_t\beta_\tau| + (1-\tau)\cdot \mathbb{1}_{(y_t < x_t\beta)}|y_t - x_t\beta_\tau|\right)$, $\tau \in (0,1)$ where $\mathbb{1}_{(\cdot)}$ denotes the indicator function, taking the value one if the condition is satisfied. Note that no distributional assumptions about the error term are required.

[13] A similar approach using factors in quantile regressions can be found in Giglio, Kelly and Pruitt (2016).

the lagged quantiles and model-specific controls that we will discuss in detail later.[14] Note that there are two distinct notions of "horizon" in our application. First, the horizon in the quantile regression h, which we keep fixed at one year and which captures how forward-looking our measure of risk is. The second notion of horizon is s in the local projection, which we vary as we trace out how risks respond at different horizons to a shock at time t. The response of quantile q_τ at time $t+s$ to a *shock* at time t is then given by θ^s_τ.

We construct the impulse-response functions by estimating the sequence of the θ^s_τ's in a series of univariate regressions for each horizon. Confidence bands are based on the bootstrap procedure described in Appendix D, which controls for serial correlation in the error terms and the estimation error in the quantiles.

At this point, it is useful to contrast our approach with another approach that aims to combine quantile regressions with local projections, an approach advocated for by Linnemann and Winkler (2016). We interpret the 10th percentile of average future IP growth as a measure of downside risk, and we then ask how this measure of risk reacts to different shocks. We study a number of shocks and find it useful to use the same quantile (or measure of risk) for all shocks we study in our local projections. Linnemann and Winkler (2016), instead, are interested in one shock only and model the quantiles *conditional on, among other things, a fiscal shock* and thus include the shock directly in the quantile regression. Linnemann and Winkler (2016) cannot distinguish between the two horizons h and s that we emphasized above (since they ask a different question, they probably would not want to).[15] An advantage of their approach is that they do not require a separate step to estimate the quantiles. An

[14]To be specific, we have $\Psi(L)^s_\tau = \Psi^s_{1,\tau}L + \Psi^s_{2,\tau}L^2 + ... + \Psi^s_{p,\tau}L^p$ so that $\Psi(L)^s_\tau$ $controls_t$ only contains p lags of the control variables. We directly interpret $shock_t$ as a measure of the shock of interest. Alternatively, one could use an instrumental variables approach. The first stage of a two-stage least squares estimation would be the same across all quantiles, so all estimates would be rescaled by the same factor. We thank a referee for pointing this out.

[15]Another approach in empirical macroeconomics that uses quantile regressions is introduced in Mumtaz and Surico (2015), who use quantile autoregressive models to study state dependence in the consumption-interest rate relationship. Recent work combining quantile regressions with VAR models to estimate impulse responses is presented in Chavleishvili and Manganelli (2017) and Kim, Lee and Mizen (2019).

advantage of our approach is that it allows us to focus on the shocks' impact on future growth that operates solely through the conditioning variables of the quantile regression (in our case, macroeconomic activity and financial conditions). We study this advantage further via Monte Carlo simulations in Appendix H. Our approach also comes with the benefit of reducing estimation uncertainty. We show this and provide a more detailed comparison of the approaches in a simple example in Appendix J.[16]

4 The Response of Tail Risk to Macroeconomic Shocks

We estimate how quantiles of average industrial production growth over the next year respond to the following aggregate shocks: a monetary shock, a financial shock, an uncertainty proxy, and an oil price shock. We choose these shocks because they represent very different sources of economic fluctuations - if the response patterns are similar across these shocks, this gives us confidence that a common propagation mechanism is at play. We identify these shocks via *standard* proxies in the literature. In particular, as much as possible we use proxies that not only have been used in the literature before, but that also can be directly computed from the data without needing to estimate an auxiliary statistical model. Next, we introduce the specifications and data transformations. More details on our data sources are provided in Appendix B. A large battery of robustness checks can be found in Appendix E. These include alternative samples, alternative monetary policy shocks, using a monthly measure of real GDP growth (Caldara *et al.*, 2020) instead of IP, and studying six-month ahead growth instead of one-year ahead growth.

All local projections are estimated using the same sample size as our quantile regression (January 1983 to December 2019), with the aforementioned exception of the monetary policy

[16] If we denote by y_t our variable of interest, x_t the vector of conditioning variables and ε_t^1 the structural shock of interest, the "one-step" approach of Linnemann and Winkler (2016) estimates quantiles of the distribution $p(y_t|x_{t-1}, \varepsilon_t^1)$. Our approach instead first estimates the quantiles of the distribution $p(y_t|x_t)$ and then estimates the effects of shocks on those quantiles.

shock, in which case we reduce the sample size for the quantile regression to align samples.

Monetary Policy Shocks Our proxy for a monetary policy shock is the surprise in the three-months ahead Fed Funds futures (Gertler and Karadi, 2015) around FOMC meetings.[17] To deal with the potential confounding issues that have been raised around high-frequency monetary surprises (see, e.g., Nakamura and Steinsson (2018), Jarociński and Karadi (2020), Miranda-Agrippino and Ricco (2021), and Zhang (2022)) we control for lagged values of both the shock and a set of macroeconomic variables in our local projections. We thus estimate the following regression for the sample February 1990 to December 2019:

$$q_{\tau,t+s} = \delta_\tau^s + \theta_t^s surprise_t + \Psi(L)_\tau^s \left[surprise_t, \Delta IP_t, \pi_t^{cpi}, \pi_t^{commodity}, i_t\right]' + u_{\tau,t+s}^s \tag{4.1}$$

where we control for twelve lags of: the monetary policy surprise $surprise_t$, industrial production growth ΔIP_t, CPI inflation π_t^{cpi}, commodity inflation $\pi_t^{commodity}$ and the federal funds rate i_t.

Credit Spread Shocks We use the Gilchrist and Zakrajšek (2012) excess bond premium (EBP) updated by Favara, Gilchrist, Lewis and Zakrajšek (2016) to construct an aggregate credit spread shock. This shock can be identified by setting the controls in the local projection appropriately.[18] For the identification of EBP shocks, we assume that no other shocks can affect the excess bond premium on impact within a month. The effect of an EBP shock is then equal to θ_τ^s because that coefficient encodes the effect of unexpected movements in the Excess Bond Premium after controlling for lags of the Excess Bond Premium, CPI inflation, IP growth, and the nominal interest rate.

[17] We follow Gürkaynak *et al.*'s (2022) construction of this surprise.

[18] For a further discussion of how timing restrictions such as this can be incorporated into local projections, see Barnichon and Brownlees (2019) and Plagborg-Møller and Wolf (2021).

We estimate the following regression for the sample from January 1983 to December 2019:

$$q_{\tau,t+s} = \delta_\tau^s + \theta_\tau^s \ EBP_t + \Psi(L)_\tau^s \ \Big[EBP_t, \ \pi_t^{cpi}, \ \Delta IP_t, \ i_t \Big]' + u_{\tau,t+s}^s, \tag{4.2}$$

where we include twelve lags of all controls.

Oil Price Shock We investigate the effects of oil price shocks on growth quantiles by using the asymmetric measure of net oil price increase proposed by Hamilton (2003). We thus define an oil price shock as the percentage increase (negative changes are censored out) in the monthly oil price over the peak experienced in the previous thirty-six months:

$$shock_{36m,t} = 100\max(0, \log p_t - \max(\log p_{t-1}, \log p_{t-2}, ..., \log p_{t-36}))$$

where p_t stands for the producer price index for crude petroleum.

We run the following local projection for the sample from January 1983 to December 2019:

$$q_{\tau,t+s} = \delta_\tau^s + \theta_\tau^s \ shock_{36m,t} + \Psi(L)_\tau^s \ \Big[shock_t, \ \pi_t^{cpi}, \ \Delta IP_t, \ i_t \Big]' + u_{\tau,t+s}^s, \tag{4.3}$$

where π_t^{cpi} is the CPI inflation rate, ΔIP_t industrial production growth and i_t the federal funds rate. We include twelve lags of the shock itself and of the control variables.

Uncertainty Shock We investigate the effects of uncertainty shocks on growth quantiles by using the uncertainty proxy constructed by Piffer and Podstawski (2018), updated to December 2019. This proxy is obtained by calculating changes in the price of gold around uncertainty events. We estimate the following local projection from January 1983 to December 2019:

$$q_{\tau,t+s} = \delta_\tau^s + \theta_t^s proxy_t + \Psi(L)_\tau^s [proxy_t, \Delta IP_t]' + u_{\tau,t+s}^s, \tag{4.4}$$

where twelve lags of the proxy and of industrial production growth ΔIP_t are included.

Summarizing Estimation Uncertainty Our approach is subject to two key sources of statistical uncertainty: not only are the coefficients in the local projections step subject to estimation uncertainty, but the quantiles that are used as data in the local projection step themselves are estimated with uncertainty. We thus design a bootstrap procedure to obtain confidence intervals that capture the uncertainty of both the quantile regression and the local projection step. The full details are provided in Appendix D.

Interquantile Ranges The uncertainty around the IRFs of single quantiles estimated in separation from each other cannot readily answer the question of whether quantile responses are statistically different from each other because they represent marginal responses that disregard the correlation between the responses of the various quantiles. This is why we estimate, for all shocks, another regression in which we recognize that the quantiles come from a common data-generating process and thus compute the impulse responses of interquantile ranges directly. The specification reads:

$$q_{\tau_1,t+s} - q_{\tau_2,t+s} = \delta_\tau^s + \theta_\tau^s \ shock_t + \Psi(L)_\tau^s \ X_t + u_{\tau,t+s}^s, \tag{4.5}$$

where τ_1 and τ_2 are the quantiles of the interquantile range and X_t the shock-specific controls.

4.1 Results

We present the impulse responses of the one-year-ahead industrial production growth quantiles and interquantile ranges in Figure 3 and Figure 4. In the top panel, we plot the impulse responses of the quantiles after a contractionary shock. To make the responses comparable across shocks, we rescale the responses across quantiles such that the median falls by 25 basis points on impact (this procedure does not distort the sign of the response). The key takeaway from Figures 3 and 4 is that there is a clear asymmetry in the response to all shocks we consider: *The 10th percentile moves more than the median, which in turn moves more* *than the 90th percentile.* The responses of the difference between the 10th and 50th quantiles are statistically different from zero, whereas the same cannot be said about the responses of the difference between the 50th and 90th quantiles.

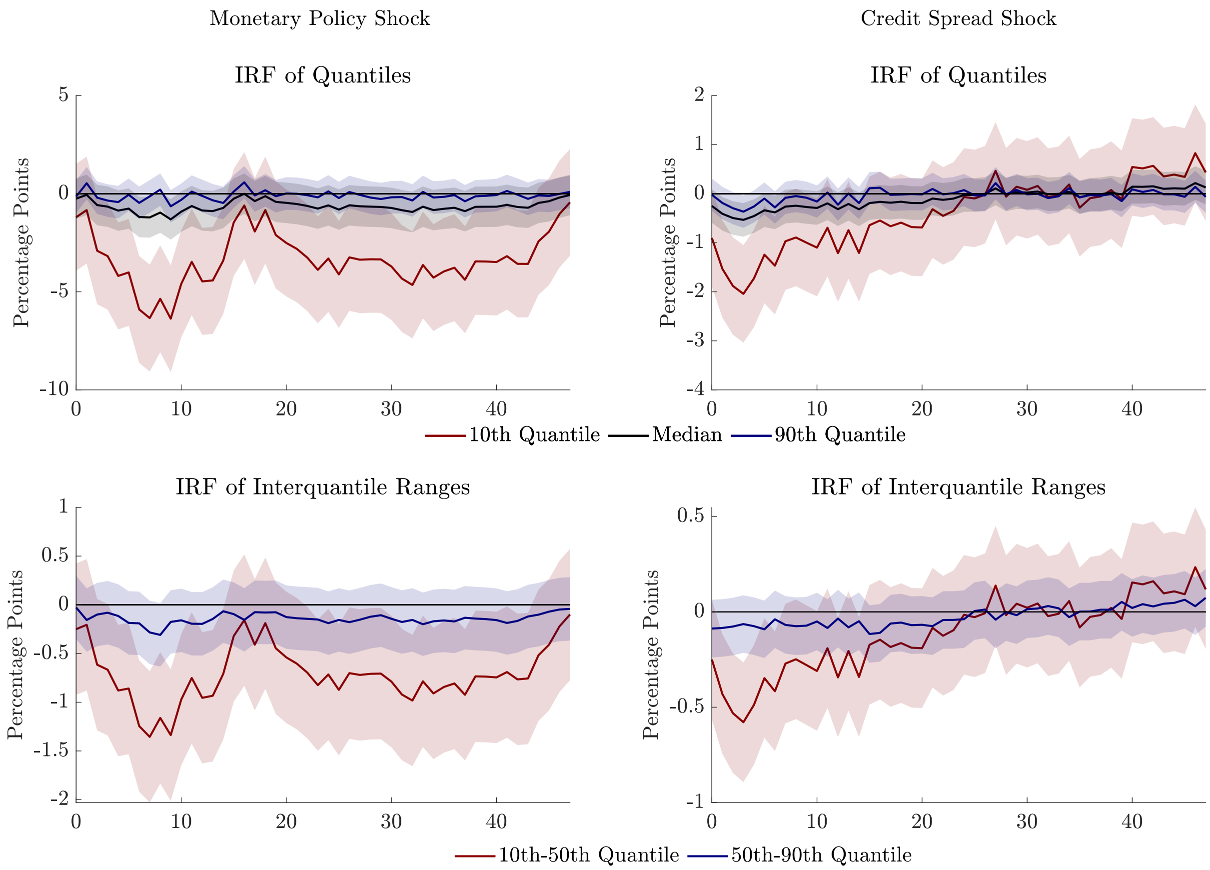

Figure 3: Impulse Responses of Quantiles of Average Industrial Production Growth over the Next Year to *Contractionary* Shocks.

Note: Red is response of the 10th quantile, black is the median response, blue is response of the 90th quantile. Confidence bands correspond to median response, 68% significance level, based on bootstrapped standard errors. The x-axis gives the horizon of the impulse response, in months. The response on the y-axis is measured in percentage points.

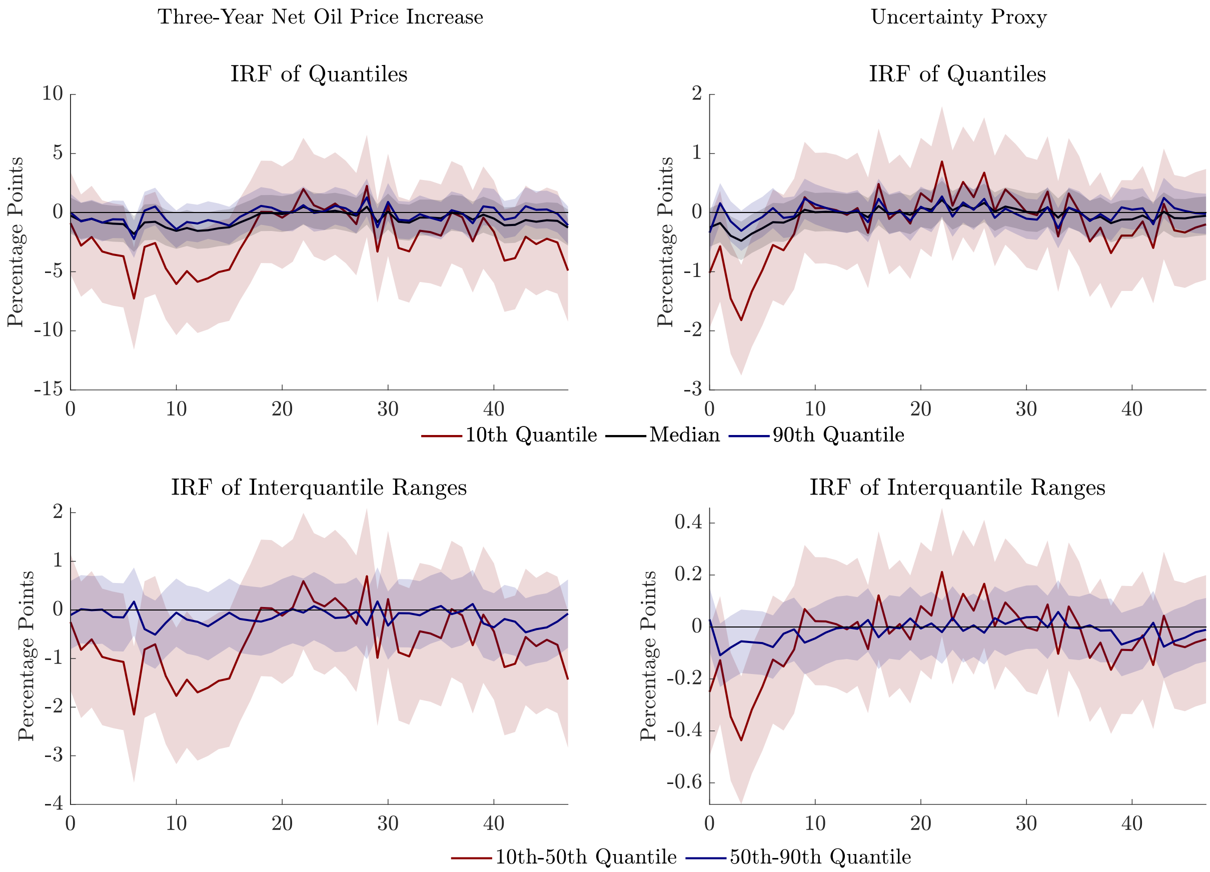

Figure 4: Impulse Responses of Quantiles of Average Industrial Production Growth over the Next Year to *Contractionary* Shocks.

Note: Red is response of the 10th quantile, black is the median response, blue is response of the 90th quantile. Confidence bands correspond to median response, 68% significance level, based on bootstrapped standard errors. The x-axis gives the horizon of the impulse response, in months. The response on the y-axis is measured in percentage points.

These differences are economically significant. To give a sense of the quantities, Table 1 shows the average ratio of the impulse responses of the 10th percentile relative to the median for the first year (in other words, we look at the value of the red line in the top panels of Figures 3 and 4 divided by the black line in the same panels).

On average, the response of the 10th percentile can be more than *three and a half* times that of the median in the first year: the average ratio is 5.9 for the monetary policy shock, 3.7 for the credit spread shock, 3.8 for the oil price shock and 4.7 for the uncertainty proxy.

Table 1: Ratio of Impulse Responses (10th Quantile to Median) Over First Year.

	Average Ratio
Monetary Policy Shock	5.9
Credit Spread Shock	3.7
Three-Year Net Oil Price Increase	3.8
Uncertainty Proxy	4.7

This means that a contractionary shock not only worsens average (median) outcomes, it also moves probability mass to the left tail of the industrial production growth distribution even relative to what one would expect from median outcomes. This statement holds true for all shocks we consider. These results stress the importance of assessing how shocks move the entire distribution of future outcomes, and not just measures of central tendency.

As we show in the next section, a linear model cannot generate this asymmetry. Hence, our results emphasize that nonlinearities are important to understand macro risk.[19] Furthermore, these nonlinearities cannot be tightly linked to the response to one specific shock, as they are present in all shocks we study. Our results thus imply that these asymmetries are a feature of the propagation mechanism of shocks. In the next section, we describe two data-generating processes that rationalize the asymmetries we find in the data.

[19] As highlighted in Koenker (2005), even linear quantile regressions such as those used here can capture nonlinearities because each quantile is modeled separately.

4.2 Inspecting the Relevance of Macro and Financial Conditions

In this section, we modify our estimation procedure to gain insight into the sources of the asymmetry in response to shocks that we established in the previous section. Specifically, in the quantile regression step (3.1) we set to zero, post estimation, the coefficients associated with industrial production growth and otherwise keep the coefficient on financial conditions unchanged when recomputing the quantiles. That is:

$$\widehat{Q}_{IP-partial,\tau}(\bar{\Delta}IP_{t+1,t+12}|NFCI_t, \Delta IP_t) = \hat{\alpha}_\tau + \hat{\beta}_\tau NFCI_t + \underbrace{\hat{\gamma}_\tau}_{=0} \Delta IP_t, \quad \tau \in (0,1) \tag{4.6}$$

These recomputed quantiles, which partial out the effect of IP growth are then passed on to the local projection step. This modification allows us to explore how important financial conditions are for the asymmetries that we find in US data.

The resulting quantiles are shown in Figure 5: They all display markedly less noise, and while the 90th quantile has become nearly constant, both the 10th quantile and the median display broadly similar paths as in the benchmark.

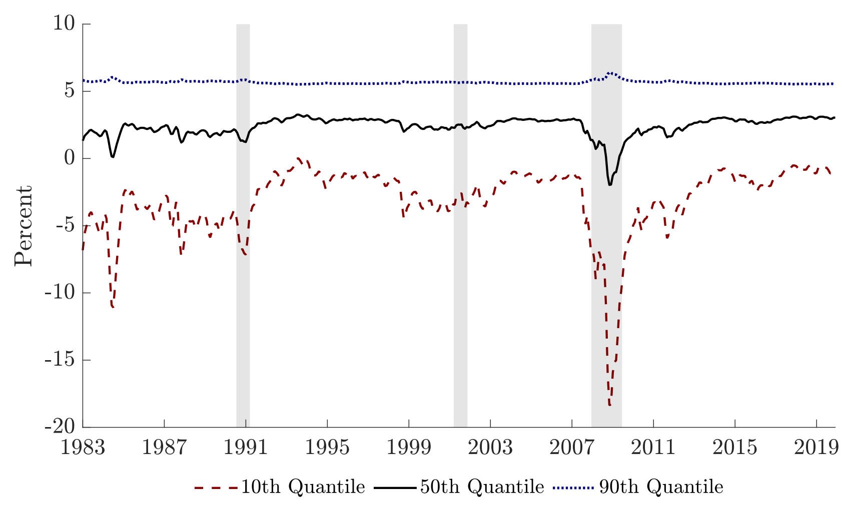

Figure 5: Quantiles of Average Industrial Production Growth over the Next Year Constructed with the Coefficients on IP Growth Set to Zero in the QR (3.1).

Note: Red is the 10th quantile, black is the median, blue is the 90th quantile. Grey-shaded bars indicate NBER-dated recessions.

Consequently, the responses of these quantiles to the four shocks obtained in the second step of the routine are also very similar to their baseline counterparts, although smoother (Figures 6 and 7). This suggests that financial conditions are essential for explaining the non-linear impact of shocks on the growth outlook.

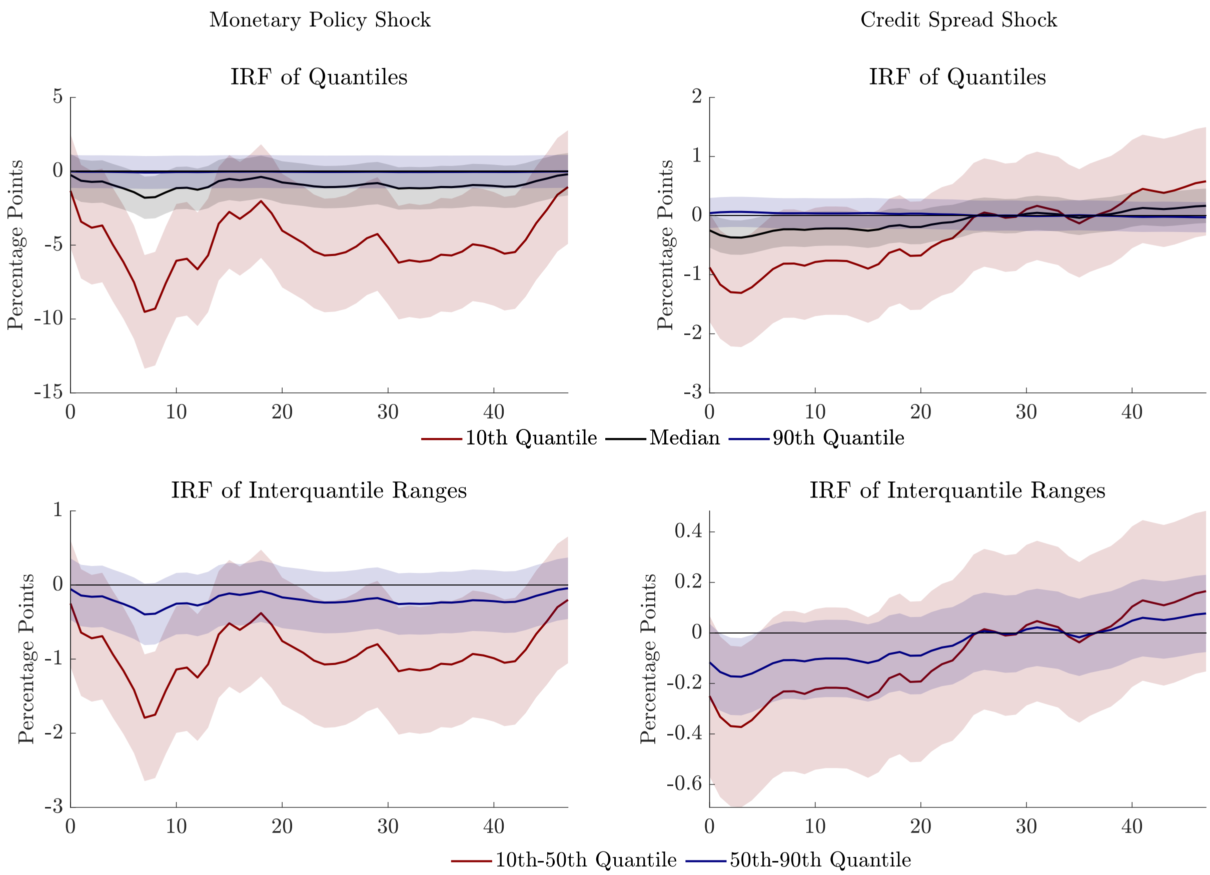

Figure 6: Impulse Responses of Quantiles of Average Industrial Production Growth over the Next Year to *Contractionary* Shocks. Quantiles are Constructed with Coefficients on IP Growth Set to Zero in the QR (3.1).

Note: Red is response of the 10th quantile, black is the median response, blue is response of the 90th quantile. Confidence bands correspond to median response, 68% significance level, based on bootstrapped standard errors. The x-axis gives the horizon of the impulse response, in months. The response on the y-axis is measured in percentage points.

This notion is supported by an analogous exercise in which the local projection step uses quantiles constructed by setting to zero the coefficients on NFCI, instead of those on IP growth, that is:

$$\widehat{Q}_{NFCI-partial,\tau}(\bar{\Delta} IP_{t+1,t+12}|NFCI_t, \Delta IP_t) = \hat{\alpha}_\tau + \underbrace{\hat{\beta}_\tau}_{=0} NFCI_t + \hat{\gamma}_\tau \Delta IP_t, \quad \tau \in (0,1) \quad (4.7)$$

This exercise supports our conclusion: Although industrial production is a source of non-linearity in its own right, this appears to be muted in comparison to the one produced by financial conditions only (Figures F-2 and F-3 in the Appendix).

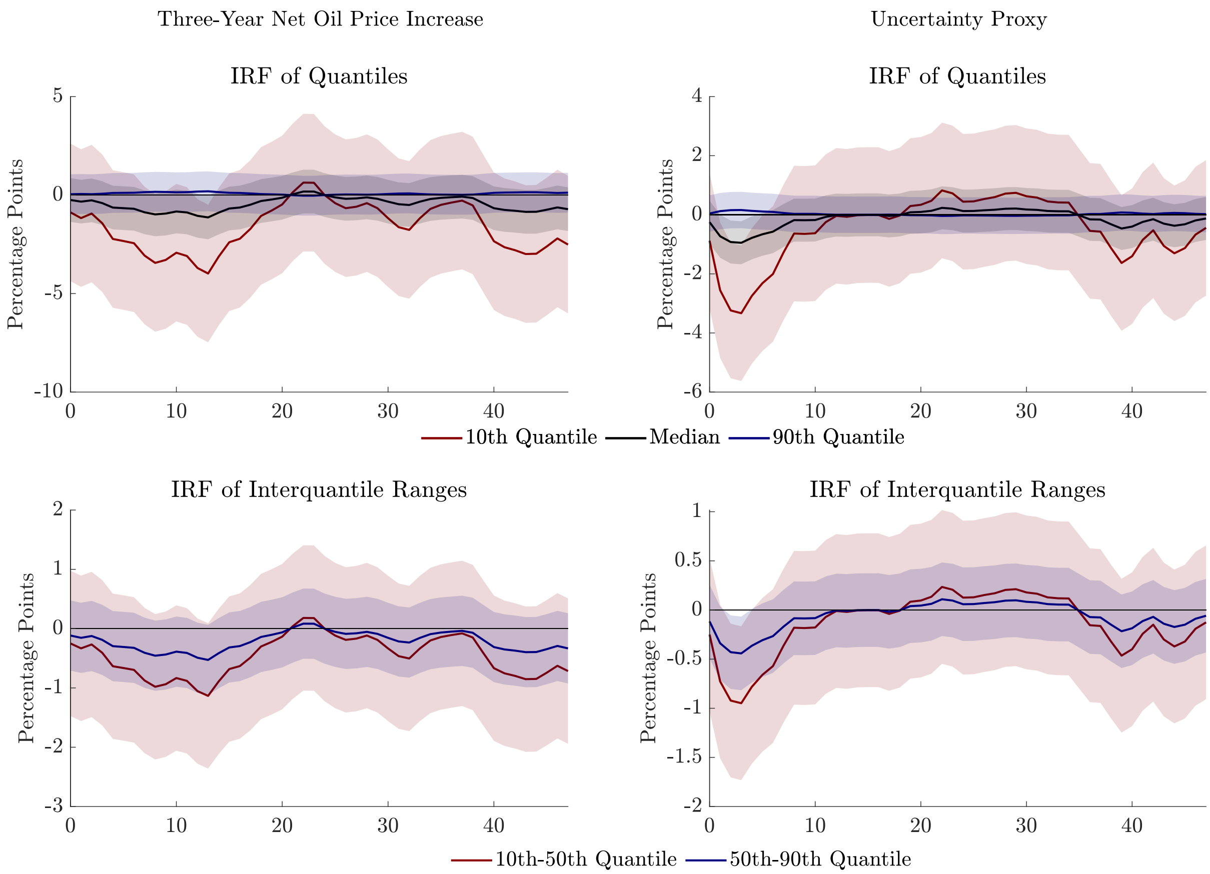

Figure 7: Impulse Responses of Quantiles of Average Industrial Production Growth over the Next Year to *Contractionary* Shocks. Quantiles are Constructed with Coefficients on NFCI Set to Zero in the QR (3.1).

Note: Red is response of the 10th quantile, black is the median response, blue is response of the 90th quantile. Confidence bands correspond to median response, 68% significance level, based on bootstrapped standard errors. The x-axis gives the horizon of the impulse response, in months. The response on the y-axis is measured in percentage points.

5 Inspecting the Economic Mechanism

As noted in our introduction, there are at least two key competing theories on the sources of Growth-at-Risk. The first is that a specific shock has an independent, nonlinear effect on growth. The second is that shocks share a common, nonlinear propagation mechanism.

In the previous section, we established that macroeconomic risk is not driven by one shock only. Indeed, we found that all shocks we consider generate an asymmetric response in the quantiles of future IP growth. In this section, we shed light on potential economic mechanisms underlying our empirical findings. As a by-product, we also validate our approach. To do so, we perform Monte Carlo experiments that draw on a "semi-structural" VAR model with switching coefficients and volatilities, as well as on the nonlinear DSGE model of Gertler, Kiyotaki and Prestipino (2019) featuring bank panics and financial accelerator mechanisms. These DGPs serve as examples that can replicate our findings. This section is *not* meant as an exhaustive description of all possible DGPs that can replicate our findings. Indeed, we do not want to take a stand on a specific DGP - our empirical approach is intentionally agnostic about the data-generating process, which we view as a strength of our approach.

5.1 A "Semi-Structural" Threshold VAR Model

We start by considering a specific version of a "semi-structural" threshold VAR model which features the following key mechanism: Whenever financial conditions and macroeconomic conditions worsen considerably, the effect of the shock on these variables is more pronounced. This reflects the idea that during recessions nonlinearities arise which exacerbate the effect of adverse shocks. We provide specific numerical values for parameters because we simulate these DGPs to evaluate our approach.

Model I *Our shock of interest "$shock_t$" has a nonlinear effect on the growth outlook through a common state-dependence governed by f_t and m_t.*

The VAR model consists of three endogenous variables and three innovations:

$$y_t = \beta_0 + \beta_1 f_t + \beta_2 m_t + \sigma_y e_t^y \tag{5.1}$$

$$f_t = \alpha_1 f_{t-1} + \alpha_2 m_t + \alpha_3(f_{t-1}, m_{t-1}) shock_t + e_t^f \tag{5.2}$$

$$m_t = \gamma_1 m_{t-1} + \gamma_2 f_{t-1} + \gamma_3(f_{t-1}, m_{t-1}) shock_t + e_t^m \tag{5.3}$$

$$\alpha_3(f_t, m_t) = \begin{cases} 5, & \text{if } f_t > f^* \ \& \ m_t < m^* \\ 1, & \text{normal state} \end{cases}, \quad \gamma_3(f_t, m_t) = \begin{cases} -5, & \text{if } f_t > f^* \ \& \ m_t < m^* \\ -1, & \text{normal state} \end{cases}$$

where y_t, f_t, m_t respectively denote the growth rate of real activity, a financial factor, and a macroeconomic factor and e_t^y, e_t^f and e_t^m are shocks to these variables; $shock_t$ is the structural shock of interest for the impulse response functions. All shocks are drawn from an independent standard normal distribution. Note that $\alpha_3(f_t, m_t)$ and $\gamma_3(f_t, m_t)$ are functions of f_t and m_t. In particular, when f_t is greater than a threshold f^* and m_t is smaller than a threshold m^* the effect of an adverse shock on future real activity growth is more pronounced. This captures the idea that due to amplification mechanisms, adverse shocks that hit during already bad times, as measured by tight financial conditions and weak macroeconomic activity, make the growth outlook particularly vulnerable. The other parameter values can be found in Appendix G.

This model encodes the view that some recessions (i.e. situations where m_t is low) can be more severe than others; for instance, if the financial variable f_t is not above the threshold, the associated recession tends to be milder. A similar idea is pursued in Jordà, Schularick and Taylor (2020). Although we focus on one structural shock here for parsimony, our results would be qualitatively the same if instead we had more than one structural shock (i.e. if we replaced $\alpha_3 shock_t$ and $\gamma_3 shock_t$ with $\sum_{i=1}^{I} \alpha_3^i shock_t^i$ and $\sum_{i=1}^{I} \gamma_3^i shock_t^i$, respectively, where $shock_t^i$ is the time t realization of the ith structural shock of interest and the number of structural shocks I is larger than 1). We show results for Monte Carlo simulations in such an environment in Appendix H.

Impulse Responses We simulate the model 1000 times for 444 periods (the number of periods between January 1983 and December 2019, as in the credit shock specification) and store $\{y_t, f_t, m_t, shock_t\}$ for each simulation. We first construct average future real activity growth over the next four periods and estimate its quantiles conditional on the financial and the macroeconomic factor. In Figure 8 we report the impulse responses of the quantiles to the (contractionary) shock of interest, computed via local projection as in our empirical exercise. We normalize the responses such that, on impact, the median drops by 25 basis points.

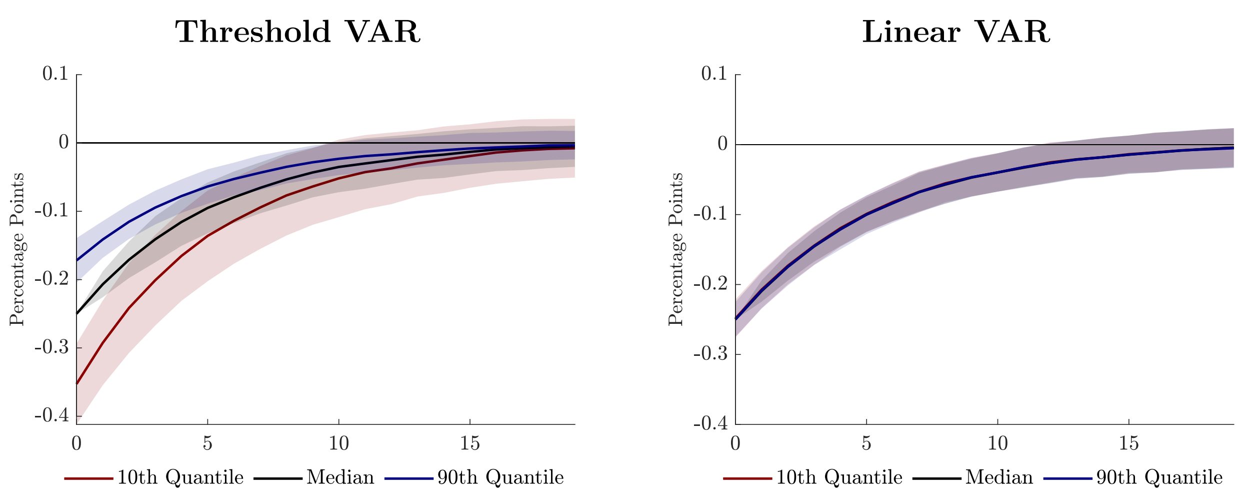

Figure 8: Impulse Responses of Quantiles of Simulated Future Real Activity Growth from Threshold VAR (Left Panel) and Linear VAR (Right Panel) Model.

Note: Straight lines are medians across simulations. Shaded areas are 68% confidence bands.

There are two important results that emerge. The first is that in the case of the threshold VAR model (left panel), the shock pushes down the left tail more strongly than other parts of the distribution, as in our empirical findings. This can be explained by the fact that when the shock hits during times of financial and macroeconomic distress, its effect is more pronounced, thus making the growth outlook more vulnerable. The second result is that, not surprisingly but reassuringly, no asymmetry is found when we shut down non-linearities in the DGP and thus consider a linear VAR model (right panel). The parameter values for the linear model can also be found in Appendix G.

Alternative Specifications of the DGP Several data-generating processes can deliver the results shown above. This happens, for instance, in model II below. In this model the shock has a linear effect on financial and macro conditions but the propagation mechanism is such that the latter are nonlinearly related to real activity growth. In particular, it features the following mechanisms. First, whenever financial conditions or macroeconomic conditions worsen, their effect on future real activity growth is more pronounced and so is its variance. (This is governed by the terms $\beta_1(f_t, m_t)$ and $\beta_2(f_t, m_t)$ in the first equation.) This reflects the idea that during recessions nonlinearities arise which can prolong and exacerbate downturns. Second, both macroeconomic and financial conditions are still driven by a common shock (structural shocks affect multiple aggregates at the same time), but this shock has a linear effect on these variables in this model.

Model II *Shock affects f_t and m_t linearly, but their effect on y_t is larger during bad times.*

$$y_t = \beta_0 + \beta_1(f_t, m_t) f_t + \beta_2(f_t, m_t) m_t + e_t^y \tag{5.4}$$

$$f_t = \alpha_1 f_{t-1} + \alpha_2 m_t + \alpha_3 shock_t + e_t^f \tag{5.5}$$

$$m_t = \gamma_1 m_{t-1} + \gamma_2 f_{t-1} + \gamma_3 shock_t + e_t^m \tag{5.6}$$

$$\beta_1(f_t, m_t) = \begin{cases} -1.5, & \text{if } f_t > f^* \;\&\; m_t < m^* \\ -0.5, & \text{normal state} \end{cases}, \quad \beta_2(f_t, m_t) = \begin{cases} 1.5, & \text{if } f_t > f^* \;\&\; m_t < m^* \\ 0.5, & \text{normal state} \end{cases},$$

If we simulate data from this competing model, use it in our estimation procedure and compute impulse responses, the model would again signal that the effect of the shock on growth is nonlinear – as evident in the right panel of Figure 9. In particular, we again obtain the result of model I, in the left panel, that the lower tail moves down more than the median. This result is not surprising since financial and macro conditions are the key variables governing the nonlinearity of future growth in our threshold VAR and both of these variables are in turn driven by that common shock.

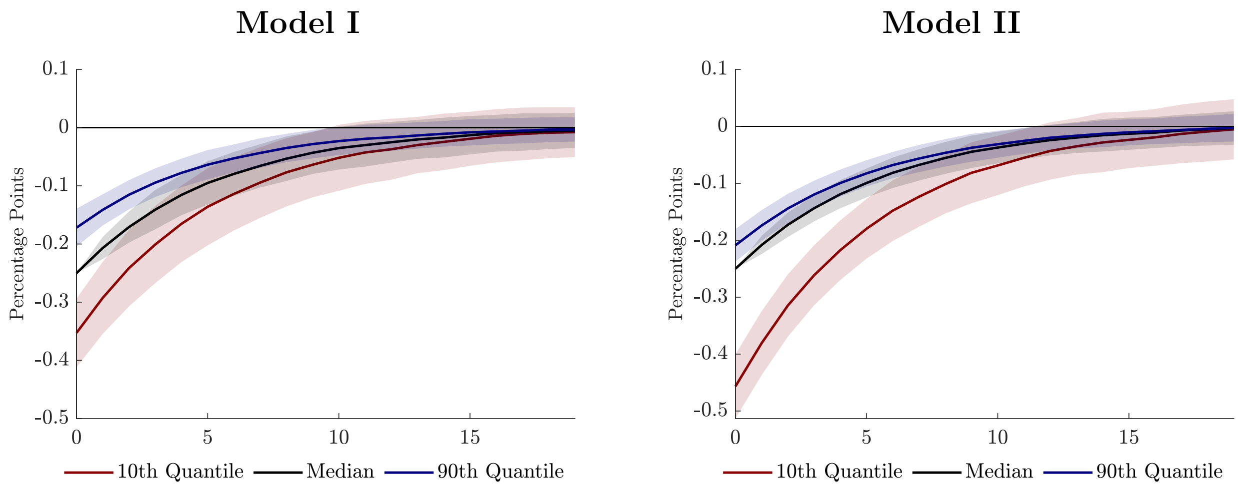

Figure 9: Comparison of Impulse Responses of Quantiles of Simulated Future Real Activity Growth from Threshold VAR. Model I vs. Model II.

Note: Straight lines are medians across simulations. Shaded areas are 68% confidence bands.

Finally, these same patterns can also be replicated by other DGPs, in which nonlinearity is modeled like in model III below, in which, once we condition on m_t, the financial factor does not feature asymmetric responses to the shock of interest - all asymmetries in this model are determined by the asymmetric response of the macro factor to the shock.[20] Model III thus acknowledges how the interdependence between macro and financial conditions can confound inference on which variables are responsible for the asymmetric response of real activity growth to shocks.

[20]Naturally, we could write down a model with the exact opposite role of factors.

As mentioned above, we think of these models as laboratories that highlight possible sources of our empirical findings. We intentionally made them as simple as possible. Nevertheless, some readers might find it useful to think about how to distinguish between these models. One possible approach is the one we take in Section 4.2, where we examine the role of the conditioning variables in the first stage quantile regression. This can help researchers understand whether all or only a subset of conditioning variables lead to asymmetries. Alternatively, one could directly study the dynamics of the conditioning variables in the quantile regressions. While correctly specified regressions for the macro and financial factors of the form (5.8) and (5.9) would asymptotically uncover the correct source of asymmetry, alternative specifications (such as a specification that replaces m_t with m_{t-1} in Equation (5.8)) could easily lead researchers astray. Telling models I and II apart is thus a daunting task.

Distinguishing between the mechanism present in model II (where nonlinearities come from the relationship between factors and output growth) and the mechanism present in models I and III (where nonlinearities come from the dynamics of the factors themselves) is instead more straightforward by either following the approach in Section 4.2 or by estimating quantile regressions of the financial and macro factors, as these regressions can tell us whether these variables exhibit nonlinearities.

Model III *Asymmetry from macroeconomic conditions m_t is inherited by f_t and y_t.*

$$y_t = \beta_0 + \beta_1 f_t + \beta_2 m_t + \sigma_y e_t^y \tag{5.7}$$

$$f_t = \alpha_1 f_{t-1} + \alpha_2 m_t + \alpha_3 shock_t + e_t^f \tag{5.8}$$

$$m_t = \gamma_1 m_{t-1} + \gamma_2 f_{t-1} + \gamma_3 (m_{t-1}) shock_t + e_t^m \tag{5.9}$$

Appendix G displays the IRFs for a variant of the threshold VAR Model II with non-constant variance as well as for Model III.

Additional Models In Appendix G we also present additional models to show how our approach, which computes conditional quantiles using quantile regression (QR) in a first step and then their dynamic responses using local projection (LP) in a second step, is useful in at least two ways. First, it can detect whether a conditioning variable is behind the asymmetry displayed by the impulse responses. Second, it can be informative as to whether the shocks propagate to the growth quantiles through a common propagation mechanism.

5.2 A Macroeconomic Model with Financial Panics

Next, we show that the nonlinear DSGE model of Gertler, Kiyotaki and Prestipino (2019) can also rationalize our empirical findings. We briefly discuss the key mechanism that generates the nonlinearity in this model. We refer interested readers to the original paper for details of the model.[21] The model is fully microfounded and extends the conventional New Keynesian model with investment by introducing bankers. Bankers are more efficient than households in handling loans. However, bankers are constrained in their ability to raise external funds and are subject to runs. The latter gives rise to multiple equilibria: one with and one without a financial panic.

A financial panic forces the banking system into liquidation, expanding the share of capital held by households. The reallocation of capital holdings from bankers to less efficient households increases the cost of capital, which ultimately disrupts firms' borrowing. Consequently, investment drops substantially more than in the equilibrium without a bank run. A self-fulfilling financial panic equilibrium exists if and only if, in the event of all other depositors' run, an individual household will be better off to follow the run. When financial conditions are strong, the economy fluctuates around a standard equilibrium. In contrast, when the financial system is weak (i.e., at the edge of the bank-run regime), even a small shock can push the economy into a self-fulfilling bank-run equilibrium. Combined with a

[21] The full model consists of 40 equations which we do not include here for the sake of brevity.

sunspot shock, this triggers a financial panic and a deep recession.

We solve the model nonlinearly using a global solution method, and then simulate 1,000 samples of the same length as our benchmark sample. With those samples in hand, we then estimate the quantile regression and the local projections as in our empirical application for each sample. We follow the original paper in focusing on a capital quality shock as a representative structural shock. Details of the model solution, simulation, as well as additional results for this model can be found in Appendix I.

Impulse Responses Figure 10 presents the impulse responses of the quantiles of log GDP (in deviation from its steady state) to the (contractionary) capital quality shock, computed as in our empirical exercise. Also in this example, we normalize the responses such that, on impact, the median drops by 25 basis points. We again find that the shock pushes down the left tail more strongly than other parts of the distribution, as in our empirical findings.

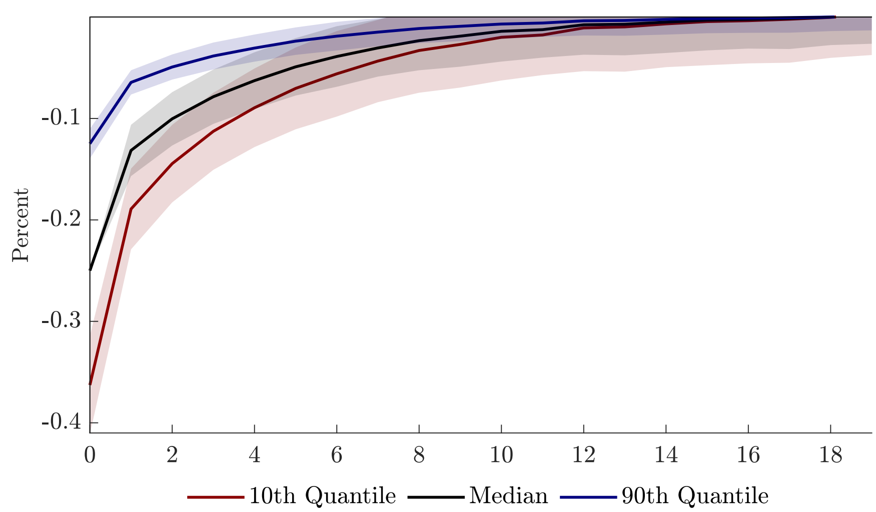

Note: Straight lines are medians across simulations. Shaded areas are 68% confidence bands.

Figure 10: Impulse Responses of Quantiles of Simulated log(GDP) to a Capital Quality Shock from Gertler, Kiyotaki and Prestipino (2019) Model.

6 Conclusion

This paper studies tail risk in U.S. aggregate outcomes. In particular, we study how macroeconomic shocks affect tail risk. All shocks considered affect tail risk disproportionately more than other quantiles (on average, the response of the 10th percentile over the first year after impact is at least 3.7 times larger than the median). Contractionary shocks thus deserve even more attention than what their effect on average outcomes suggests to the extent that they make poor economic conditions more likely. Our results suggest that policymakers should be especially weary of unexpected adverse changes in the economy.

The fact that all shocks we study display this tail-risk asymmetry points to a common mechanism lying behind these asymmetries. Indeed, the two data-generating processes we use as laboratories to test this hypothesis can replicate our findings: In the first experiment, a threshold VAR model, a common mechanism (which could be thought of as a financial accelerator mechanism in a more structural model) amplifies the negative effect on economic growth of a deterioration in financial and macroeconomic conditions. In the second, a macroeconomic model with financial panics, the bank-run equilibrium features nonlinearities that magnify the effects of a financial panic on economic activity. Consequently, we argue that nonlinear equilibrium models are necessary for modeling and studying macroeconomic risk. Our paper helps researchers in this endeavor by presenting stylized facts on asymmetric effects of shocks that researchers can use to calibrate their models.

References

Adrian, T., Boyarchenko, N. and Giannone, D. (2019). Vulnerable Growth. *American Economic Review*, **109** (4), 1263–1289.

—, Liang, N., Zabczyk, P. and Duarte, F. (2020). *Monetary and Macroprudential Policy with Endogenous Risk*. IMF Working Papers 2020/236, International Monetary Fund.

Aikman, D., Bluwstein, K. and Karmakar, S. (2021). *A tail of three occasionally-binding constraints: a modelling approach to GDP-at-Risk*. Bank of England working papers 931, Bank of England.

Barnichon, R. and Brownlees, C. (2019). Impulse Response Estimation by Smooth Local Projections. *The Review of Economics and Statistics*, **101** (3), 522–530.

—, Matthes, C. and Ziegenbein, A. (2022). Are the Effects of Financial Market Disruptions Big or Small? *The Review of Economics and Statistics*, **104** (3), 557–570.

Caldara, D., Cascaldi-Garcia, D., Cuba Borda, P. and Loria, F. (2020). Understanding Growth-at-Risk: A Markov-Switching Approach. *mimeo*.

Carriero, A., Clark, T. E. and Marcellino, M. (2020). *Capturing Macroeconomic Tail Risks with Bayesian Vector Autoregressions*. Working Papers 202002, Federal Reserve Bank of Cleveland.

Chavleishvili, S. and Manganelli, S. (2017). Quantile Impulse Response Functions.

Cogley, T. and Sargent, T. J. (2005). Drift and Volatilities: Monetary Policies and Outcomes in the Post WWII U.S. *Review of Economic Dynamics*, **8** (2), 262–302.

Cúrdia, V., Del Negro, M. and Greenwald, D. L. (2014). Rare Shocks, Great Recessions. *Journal of Applied Econometrics*, **29** (7), 1031–1052.

Fagiolo, G., Napoletano, M. and Roventini, A. (2008). Are Output Growth-Rate Distributions Fat-Tailed? Some Evidence from OECD Countries. *Journal of Applied Econometrics*, **23** (5), 639–669.

Favara, G., Gilchrist, S., Lewis, K. F. and Zakrajšek, E. (2016). Updating the Recession Risk and the Excess Bond Premium. (2016-10-06).

Forni, M., Gambetti, L., Maffei-Faccioli, N. and Sala, L. (2022). *Nonlinear transmission of financial shocks: Some new evidence*. Working Paper 2022/3, Norges Bank.

Gertler, M. and Karadi, P. (2015). Monetary Policy Surprises, Credit Costs, and Economic Activity. *American Economic Journal: Macroeconomics*, **7** (1), 44–76.

—, Kiyotaki, N. and Prestipino, A. (2019). A Macroeconomic Model with Financial Panics. *The Review of Economic Studies*, **87** (1), 240–288.

Giglio, S., Kelly, B. and Pruitt, S. (2016). Systemic risk and the macroeconomy: An empirical evaluation. *Journal of Financial Economics*, **119** (3), 457 – 471.

Gilchrist, S. and Zakrajšek, E. (2012). Credit Spreads and Business Cycle Fluctuations. *American Economic Review*, **102** (4), 1692–1720.

Gürkaynak, R., Karasoy-can, H. G. and Lee, S. S. (2022). Stock market's assessment of monetary policy transmission: The cash flow effect. *The Journal of Finance*, **77** (4), 2375–2421.

Hamilton, J. D. (2003). What is an oil shock? *Journal of Econometrics*, **113** (2), 363–398.

— (2011). Nonlinearities and the macroeconomic effects of oil prices. *Macroeconomic Dynamics*, **15** (S3), 364–378.

JAROCIŃSKI, M. and KARADI, P. (2020). Deconstructing Monetary Policy Surprises-the role of Information Shocks. *American Economic Journal: Macroeconomics*, **12** (2), 1–43.

JORDÀ, O. (2005). Estimation and Inference of Impulse Responses by Local Projections. *American Economic Review*, **95** (1), 161–182.

JORDÀ, O., SCHULARICK, M. and TAYLOR, A. M. (2020). *Disasters Everywhere: The Costs of Business Cycles Reconsidered*. Working Paper 26962, National Bureau of Economic Research.

JUSTINIANO, A. and PRIMICERI, G. E. (2008). The Time-Varying Volatility of Macroeconomic Fluctuations. *American Economic Review*, **98** (3), 604–641.

KILIAN, L. and MANGANELLI, S. (2008). The Central Banker as a Risk Manager: Estimating the Federal Reserve's Preferences under Greenspan. *Journal of Money, Credit and Banking*, **40** (6), 1103–1129.

KIM, T.-H., LEE, D. J. and MIZEN, P. (2019). Impulse Response Analysis in Conditional Quantile Models and an Application to Monetary Policy.

KOENKER, R. (2005). *Quantile Regression*. Econometric Society Monographs, Cambridge University Press.

— and BASSETT, G. (1978). Regression Quantiles. *Econometrica*, **46** (1), 33–50.

LINNEMANN, L. and WINKLER, R. (2016). Estimating Nonlinear Effects of Fiscal Policy Using Quantile Regression Methods. *Oxford Economic Papers*, **68** (4), 1120–1145.

MIRANDA-AGRIPPINO, S. and RICCO, G. (2021). The Transmission of Monetary Policy Shocks. *American Economic Journal: Macroeconomics*, **13** (3), 74–107.

Mumtaz, H. and Surico, P. (2015). The Transmission Mechanism In Good And Bad Times. *International Economic Review*, **56**, 1237–1260.

Nakamura, E. and Steinsson, J. (2018). High-frequency Identification of Monetary Non-neutrality: the Information Effect. *The Quarterly Journal of Economics*, **133** (3), 1283–1330.

Newey, W. K. and West, K. D. (1987). A Simple, Positive Semi-Definite, Heteroskedasticity and Autocorrelation Consistent Covariance Matrix. *Econometrica*, **55** (3), 703–708.

Piffer, M. and Podstawski, M. (2018). Identifying uncertainty shocks using the price of gold. *The Economic Journal*, **128** (616), 3266–3284.

Plagborg-Møller, M. and Wolf, C. K. (2021). Local projections and VARs estimate the same impulse responses. *Econometrica*, **89** (2), 955–980.

Politis, D. N. and Romano, J. P. (1994). The Stationary Bootstrap. *Journal of the American Statistical Association*, **89** (428), 1303–1313.

Primiceri, G. E. (2005). Time Varying Structural Vector Autoregressions and Monetary Policy. *Review of Economic Studies*, **72** (3), 821–852.

Tenreyro, S. and Thwaites, G. (2016). Pushing on a string: Us monetary policy is less powerful in recessions. *American Economic Journal: Macroeconomics*, **8** (4), 43–74.

Zhang, D. (2022). Term structure, forecast revision, and the signaling channel of monetary policy. *Journal of the European Economic Association*, **20** (4), 1522–1553.

A Some Additional Intuition for Impulse Responses of Quantiles

Next, we show an example in which the impulse responses of the quantiles cross. By construction, however, the quantiles themselves cannot cross because we directly model changes in the entire distribution. The example is similar to the first example from the main text, but we change the sequence of variances for the Gaussian distribution to achieve the crossing of the impulse responses of the 10th and 90th percentiles.

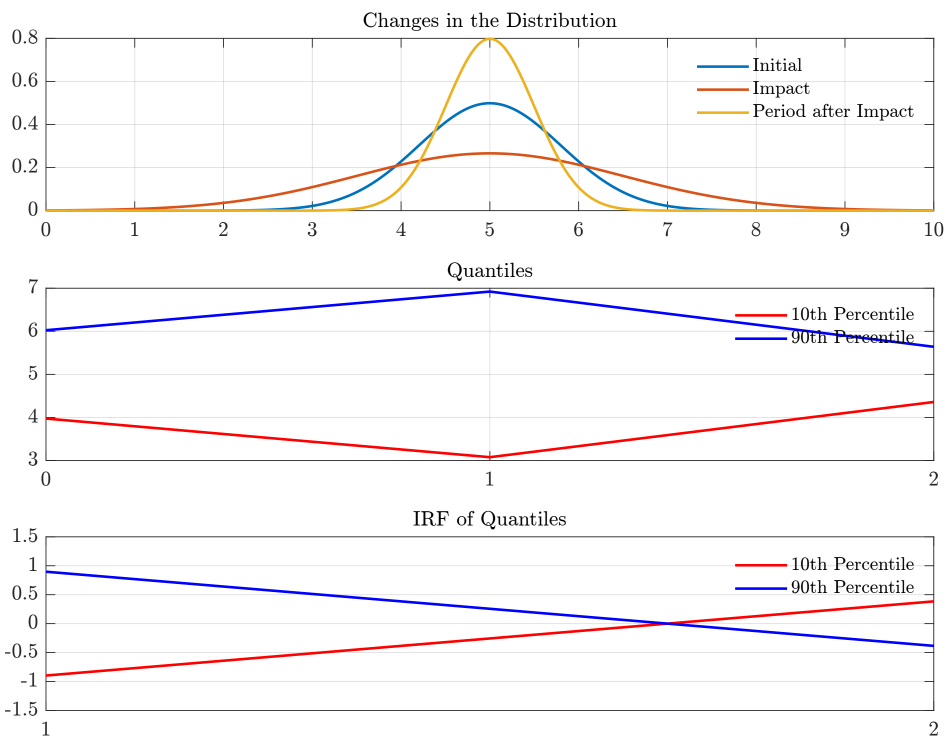

Figure A-1: Example Where Impulse Responses Cross But Quantiles Don't.

B Data

This section gives a brief overview of the data we use throughout this paper.

B.1 Growth-at-Risk Data

In the quantile regression, industrial production growth (Figure B-1) serves both as the dependent variable and as a conditioning variable alongside the National Financial Conditions Index of the Chicago Fed (Figure B-2). Both series can be retrieved from FRED (Mnemonics: INDPRO; NFCI). For Figures E-5 and E-6, we use a measure of monthly GDP growth constructed by Caldara, Cascaldi-Garcia, Cuba Borda and Loria (2020) instead of industrial production growth, both at the quantile regression stage and at the local projection stage.

Figure B-1: Dependent and Conditioning Variable in the Quantile Regression.

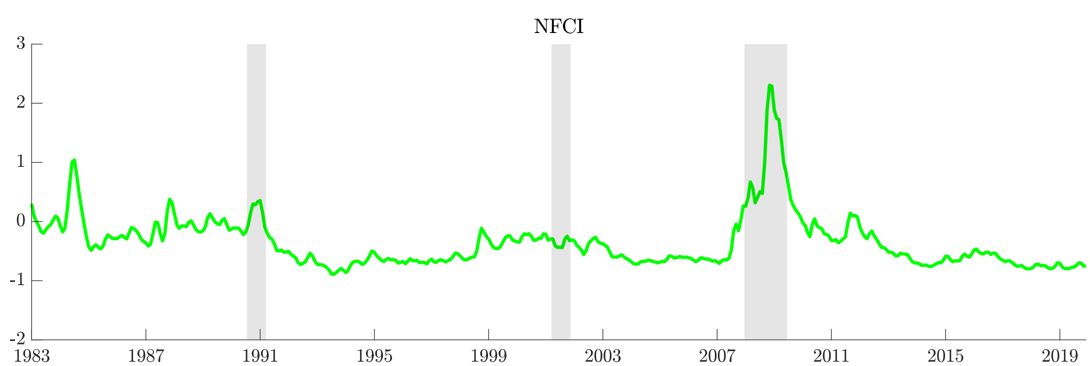

Figure B-2: Second Conditioning Variable in the Quantile Regression.

B.2 Local Projection Variables

The series of high-frequency surprises in the fourth Federal Funds Futures around FOMC meetings was provided by the Federal Reserve's Division of Monetary Affairs. Multiple observations within the same month are summed up. The excess bond premium is taken from Favara, Gilchrist, Lewis and Zakrajšek (2016)[22]. We construct the oil price shock using the Producer Price Index by Commodity: Fuels and Related Products and Power: Crude Petroleum, taken from FRED (Mnemonic: WPU0561). The uncertainty proxy is taken from Piffer and Podstawski (2018)[23]. The monetary shocks used in Figure E-9 are the Federal Funds rate shock and the policy news shock around all FOMC meetings taken from Nakamura and Steinsson (2018)[24]. Multiple observations within the same month are summed up.

Most control variables used in the local projection stage are available in FRED. The source data are:

- Consumer Price Index for all Urban Consumers: All Items.
  FRED Mnemonic: CPIAUCSL.
- Federal funds rate. FRED Mnemonic: FEDFUNDS.
- Industrial production. FRED Mnemonic: INDPRO.
- CRB Commodity Index. Haver Mnemonic: PZALL@USECON.

[22] The series can be downloaded at https://www.federalreserve.gov/econresdata/notes/feds-notes/2016/updating-the-recession-risk-and-the-excess-bond-premium-20161006.html.

[23] The authors provide an updated series at https://sites.google.com/site/michelepiffereconomics/research-1?authuser=0.

[24] We use the 1995-2014 series, which can be downloaded at https://eml.berkeley.edu/~enakamura/papers.html

B.3 Shocks

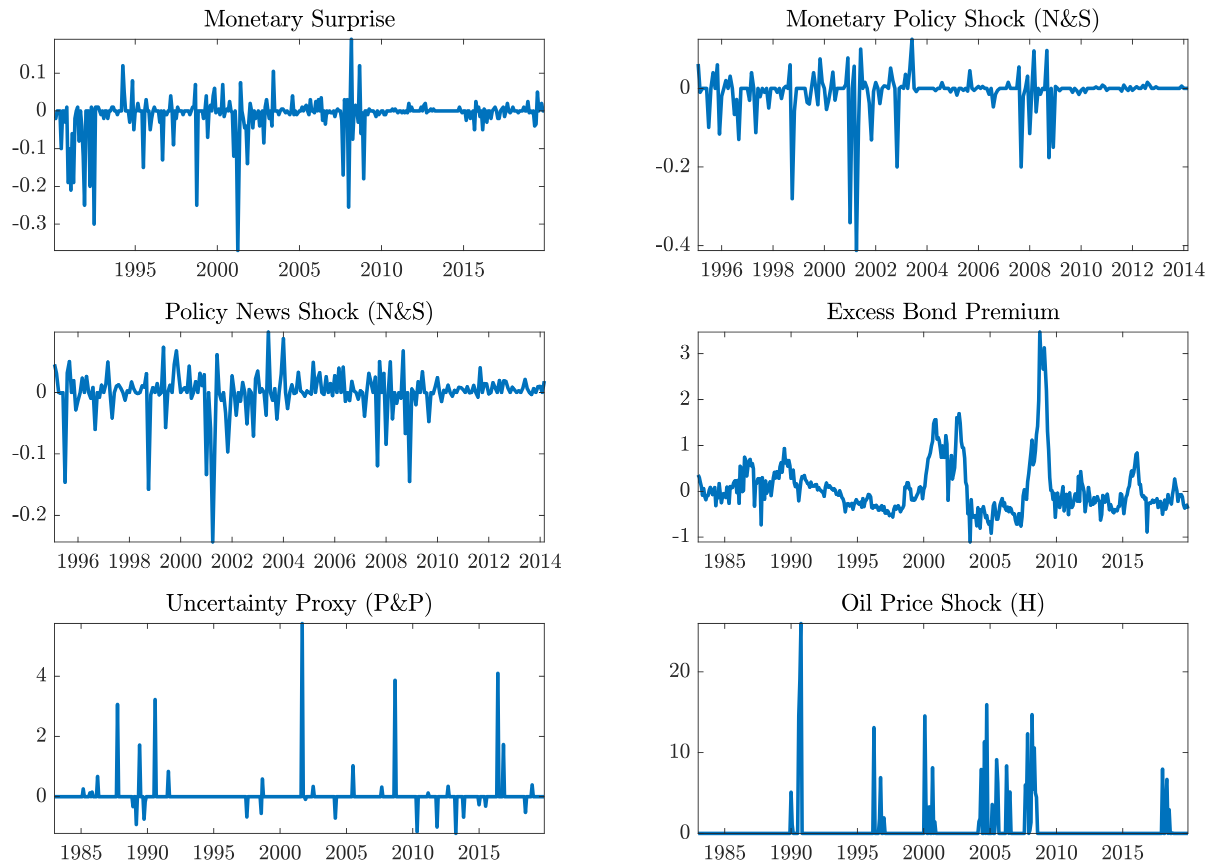

Note: The Excess Bond Premium as plotted here is itself not a proxy for a shock, but is used to construct a proxy for the EBP shock, see Equation (4.2).

Figure B-3: Shocks and Proxies.

	MS	*MPS*	*PNS*	*EBP*	*UP*	*OPS*
Monetary Surprise	1					
Monetary Policy Shock (N&S)	0.82	1				
Policy News Shock (N&S)	0.89	0.80	1			
Excess Bond Premium	-0.13	-0.13	-0.19	1		
Uncertainty Proxy (P&P)	0.05	0.07	0.06	0.17	1	
Oil Price Shock (H)	0.11	0.00	0.03	-0.01	0.02	1

Note: Common sample is February 1995 to March 2014.

Table B-1: Correlations Between Shocks (and the EBP).

C First Stage QR Estimates: Equation (3.1)

Table C-1: Quantile Regression Estimates (January 1983 - December 2019). Standard Errors in Parentheses.

	Dependent variable: Average of Industrial Production Growth over the Next Year		
	10th Quantile	Median	90th Quantile
	(1)	(2)	(3)
NFCI	-5.747^{***}	-1.636^{***}	0.278
	(1.931)	(0.531)	(0.688)
Industrial Production Growth	0.245^{***}	0.056^{**}	0.117^{***}
	(0.049)	(0.025)	(0.039)
Constant	-5.114^{***}	1.808^{***}	5.758^{***}
	(1.113)	(0.307)	(0.383)
Observations	432	432	432
Note:			*p<0.1; **p<0.05; ***p<0.01

Table C-2: Quantile Regression Estimates (February 1990 - December 2019). Standard Errors in Parentheses.

	Dependent variable: Average of Industrial Production Growth over the Next Year		
	10th Quantile	Median	90th Quantile
	(1)	(2)	(3)
NFCI	-10.681^{***}	-2.010^{**}	-0.090
	(1.908)	(0.942)	(0.700)
Industrial Production Growth	0.163^{***}	0.043	0.066^{*}
	(0.061)	(0.030)	(0.036)
Constant	-8.381^{***}	1.652^{***}	5.368^{***}
	(1.161)	(0.559)	(0.444)
Observations	347	347	347
Note:			*p<0.1; **p<0.05; ***p<0.01

D Bootstrap Procedure

This section gives a brief overview of the bootstrap procedure used to obtain the confidence bands. The procedure is designed to capture the uncertainty involved both with the quantile regression and with the local projection step of our estimation approach.

Quantile Regression Step The first step of the bootstrap procedure involves quantifying the uncertainty around the quantile regression estimates. To do so, we use the stationary "blocks-of-blocks" bootstrap of Politis and Romano (1994). For a total number of $K = 100$ bootstrap replications, blocks of data are randomly drawn to form a new sample of the same size as the original data. Importantly, the blocks are resampled in the same order for both the dependent variable y and the regressors X, a key step which preserves the time-dependency in the data. The procedure is asymptotically valid for stationary processes if the block size l increases at a suitable rate as $T \to \infty$. We set $m = \sqrt[3]{T}$, where T is the sample size. Finally, this bootstrap procedure preserves the quantile regression feature of being agnostic about the underlying distribution of the error terms, as this is not a residual-based approach.

Local Projection Step For each resampled dataset of quantiles obtained in the previous step, we now estimate a local projection for each horizon. The local projection coefficient $\hat{\theta}^s_{\tau,k}$ then captures the effect of the shock on the quantile τ at horizon s, for each bootstrap replication k. To incorporate estimation uncertainty at this second stage, we obtain 100 parameter values for the local projection parameters for each k by drawing the impulse response coefficients from their asymptotic distribution. This distribution is known and given by $\theta^s_\tau \sim \mathcal{N}\left(\hat{\theta}^s_{\tau,k}, \widehat{\Sigma}^s_{u,k}\right)$, where $\hat{\theta}^s_{\tau,k}$ is the point estimate for bootstrap sample k and $\widehat{\Sigma}^s_{u,k}$ is the estimated variance-covariance matrix of the local projection residuals $u^s_{t+s,k}$ in sample k, estimated by Newey and West (1987) with lag order $s-1$ due to the serial correlation in the error term induced by the successive leading of the dependent variable in the s-step ahead direct forecasting regression.

Combining the Uncertainty We collect all draws for one specific impulse response coefficient (pooling draws across all bootstrap samples). 68 percent confidence intervals are constructed by looking at the 16th and 84th percentile of that distribution. These intervals are then centered around the point estimate $\hat{\theta}_{\tau}^{s}$ obtained with the original sample.

Decomposing the Uncertainty In Figure D-1 we decompose the uncertainty of the growth quantiles responses to a monetary policy shock presented in Figure 3. The first set of bands (darkest color) captures local projection uncertainty only, the second set quantile regression uncertainty only, while the third combines the LP and QR uncertainty into one following our procedure.

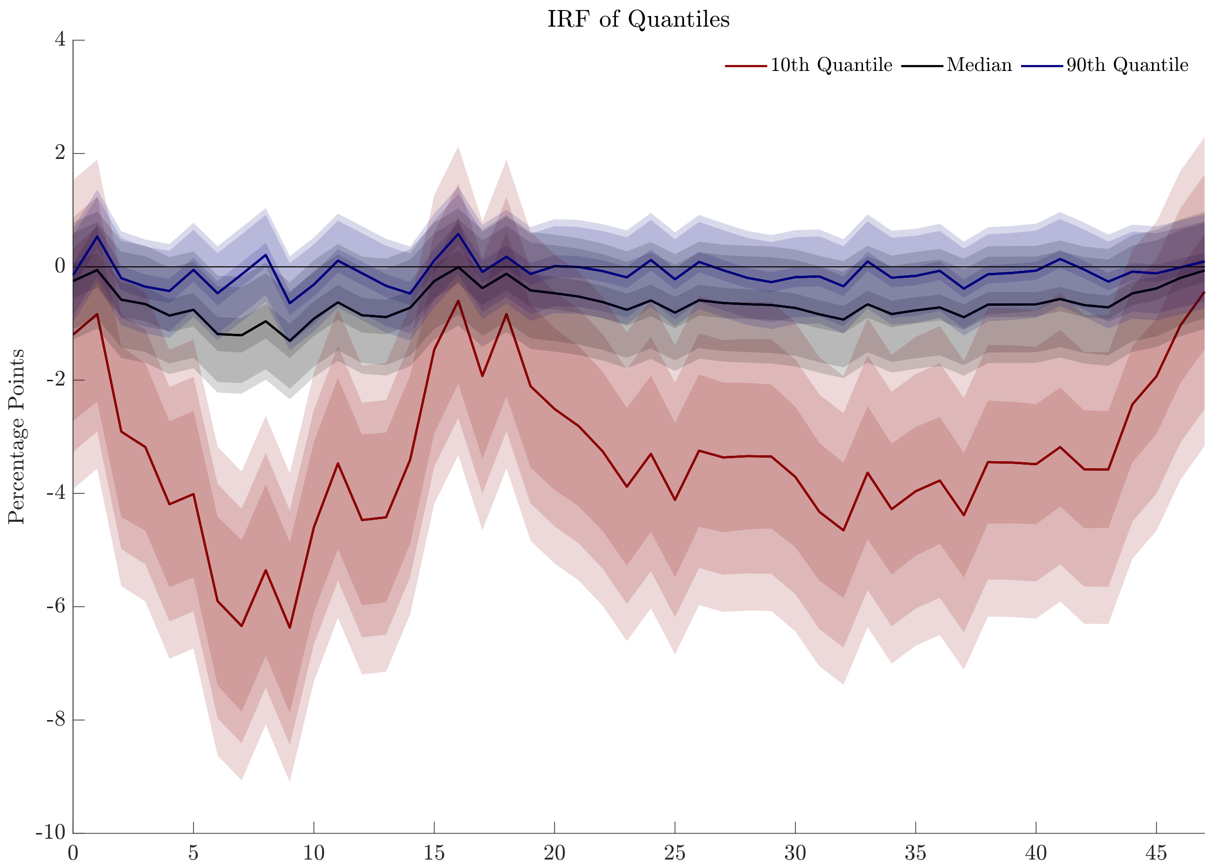

Figure D-1: Impulse Responses of Quantiles of Average Industrial Production Growth over the Next Year to *Contractionary* Shocks. Uncertainty Decomposition.

Note: Red is response of the 10th quantile, black is the median response, blue is response of the 90th quantile. Confidence bands correspond to median response, 68% significance level, based on bootstrapped standard errors. The x-axis gives the horizon of the impulse response, in months. The response on the y-axis is measured in percentage points. The first set of bands captures LP uncertainty, the second QR uncertainty, and the last combines these two uncertainties following our bootstrap procedure.

E Robustness

Below we list details on all the robustness checks in this section. Throughout, we find the same asymmetry that is present in our benchmark analysis.

Horizon - Average Industrial Production Growth over the Next Six Months We explore the sensitivity of our results to the choice of a shorter horizon for the growth outlook. In particular, we replicate our results for the choice of average industrial production growth over the next six months as a dependent variable in the quantile regression. Figures E-1 and E-2.

Starting the Quantile Regression in 1973 For the IRFs in Figure E-3 and E-4 the quantile regression starts in 1973 instead of 1983 (instead of 1990 in the case of the monetary policy shock).

Monthly GDP Instead of Industrial Production In Figures E-5 and E-6 we explore the sensitivity of our baseline results to the choice of the dependent variable. In particular, we replace the (month-over-month) growth in industrial production by monthly GDP growth as estimated by Caldara *et al.* (2020).

Pre-Great-Recession Sample Local projection stops in September 2007. See Figures E-7 and E-8.

Alternative Monetary Shocks Figure E-9 displays the IRFs to alternative monetary policy shocks.

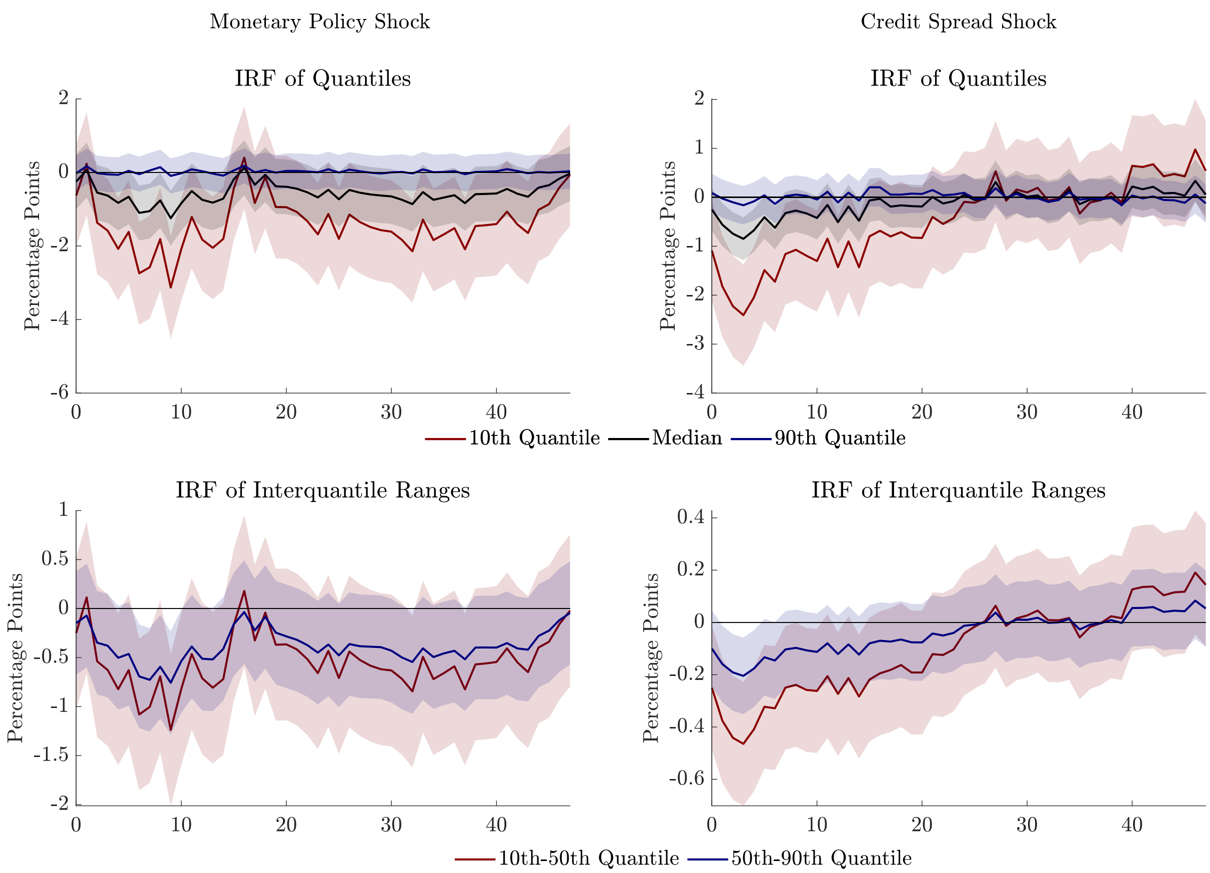

Figure E-1: Impulse Responses of Quantiles of Average Industrial Production Growth over the Next Six Months to *Contractionary* Shocks.

Note: Red is response of the 10th quantile - 50th quantile, blue is response of the 50th-90th quantile. Confidence bands correspond to median response, 68% significance level, based on bootstrapped standard errors. The x-axis gives the horizon of the impulse response, in months. The response on the y-axis is measured in percentage points.

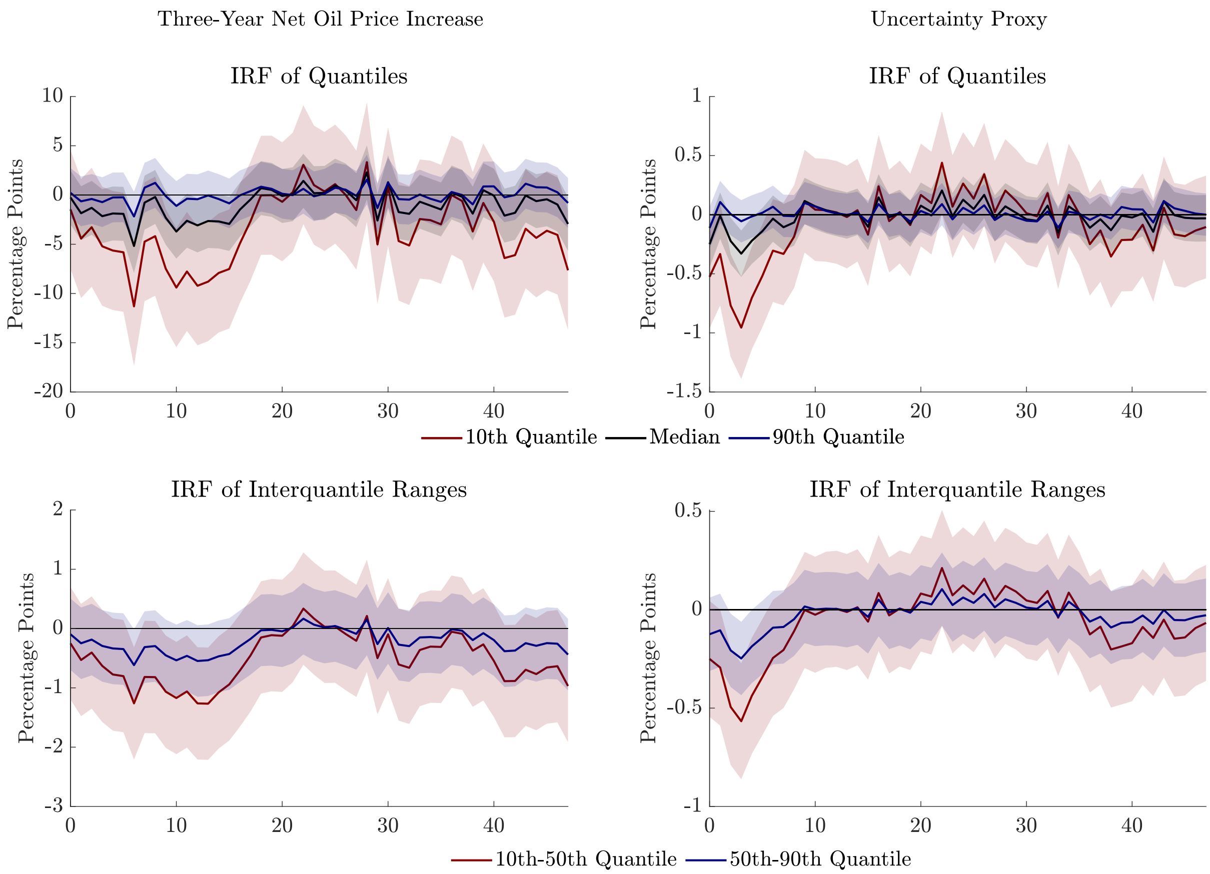

Figure E-2: Impulse Responses of Quantiles of Average Industrial Production Growth over the Next Six Months to *Contractionary* Shocks.

Note: Red is response of the 10th quantile - 50th quantile, blue is response of the 50th-90th quantile. Confidence bands correspond to median response, 68% significance level, based on bootstrapped standard errors. The x-axis gives the horizon of the impulse response, in months. The response on the y-axis is measured in percentage points.

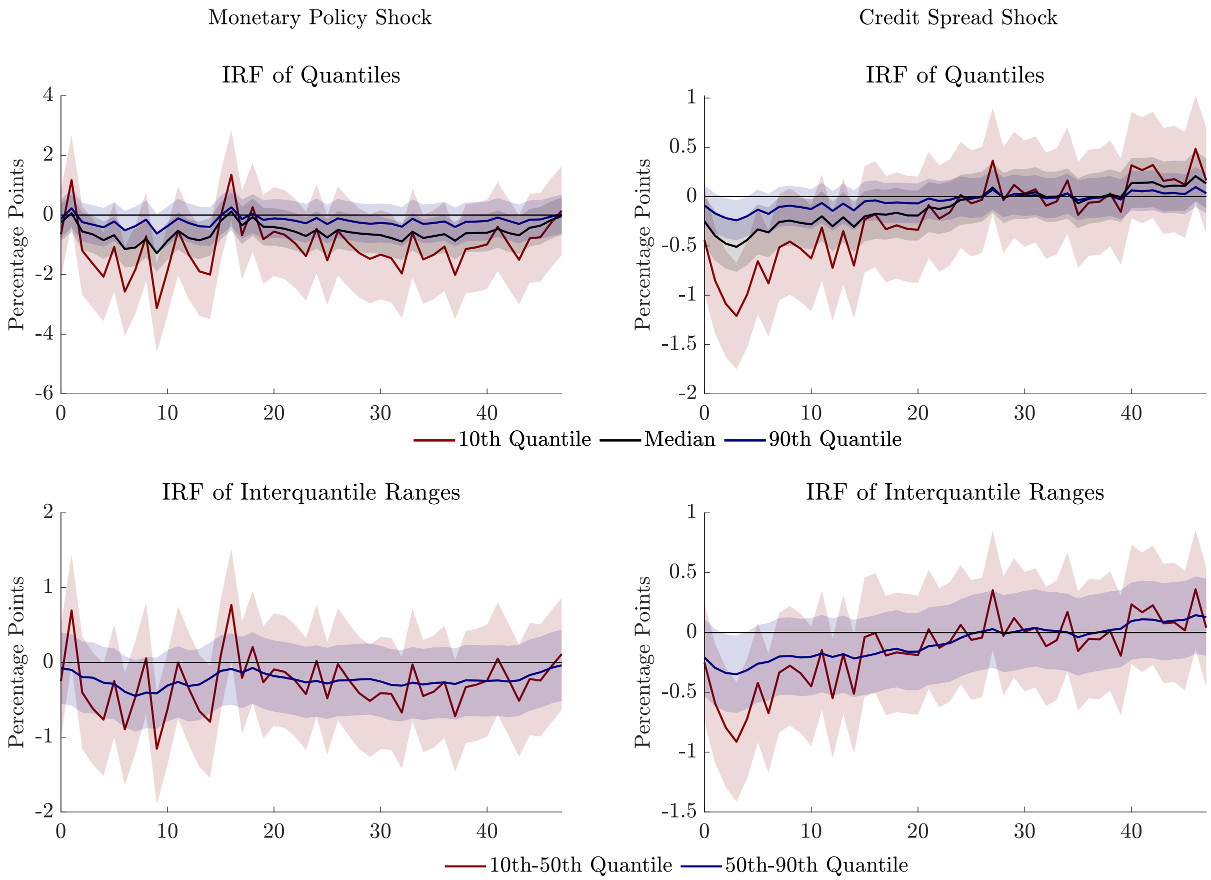

Figure E-3: Impulse Responses of Quantiles of Average Industrial Production Growth over the Next Twelve Months to *Contractionary* Shocks. Estimation of Quantile Regression Starts in 1973.

Note: Red is response of the 10th quantile - 50th quantile, blue is response of the 50th-90th quantile. Confidence bands correspond to median response, 68% significance level, based on bootstrapped standard errors. The x-axis gives the horizon of the impulse response, in months. The response on the y-axis is measured in percentage points.

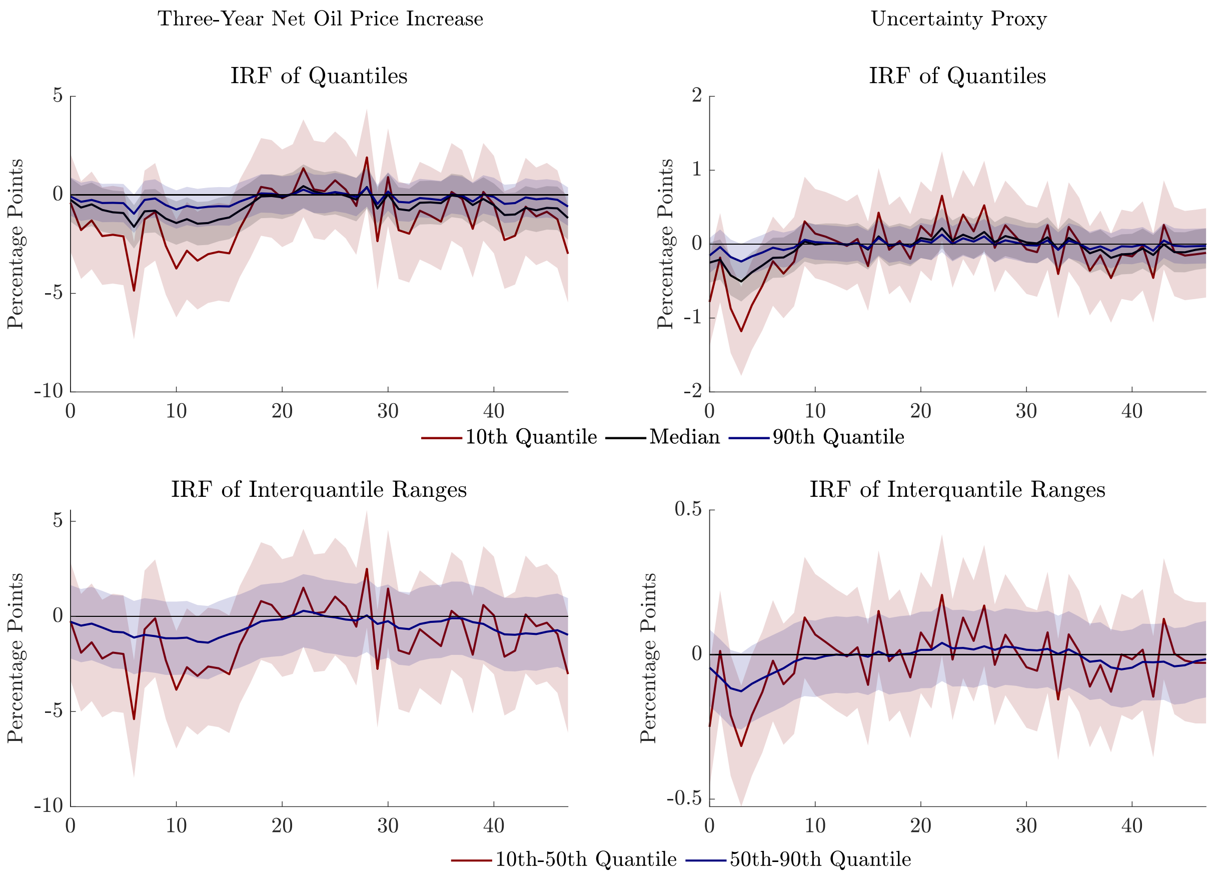

Figure E-4: Impulse Responses of Quantiles of Average Industrial Production Growth over the Next Twelve Months to *Contractionary* Shocks. Estimation of Quantile Regression Starts in 1973.

Note: Red is response of the 10th quantile - 50th quantile, blue is response of the 50th-90th quantile. Confidence bands correspond to median response, 68% significance level, based on bootstrapped standard errors. The x-axis gives the horizon of the impulse response, in months. The response on the y-axis is measured in percentage points.

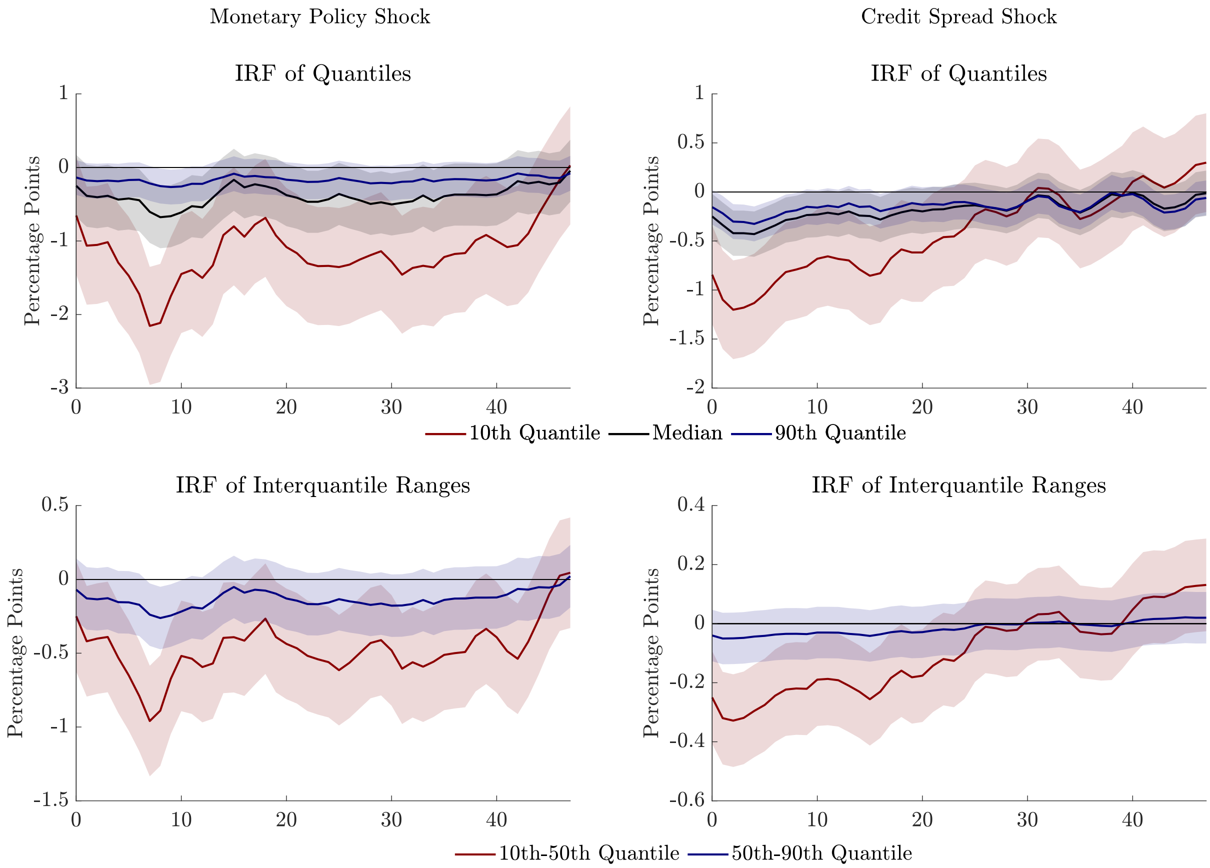

Figure E-5: Impulse Responses of Quantiles of Average GDP Growth over the Next Year to *Contractionary* Shocks. Specification using Monthly GDP Instead of Industrial Production as Dependent Variable.

Note: Red is response of the 10th quantile - 50th quantile, blue is response of the 50th-90th quantile. Confidence bands correspond to median response, 68% significance level, based on bootstrapped standard errors. The x-axis gives the horizon of the impulse response, in months. The response on the y-axis is measured in percentage points.

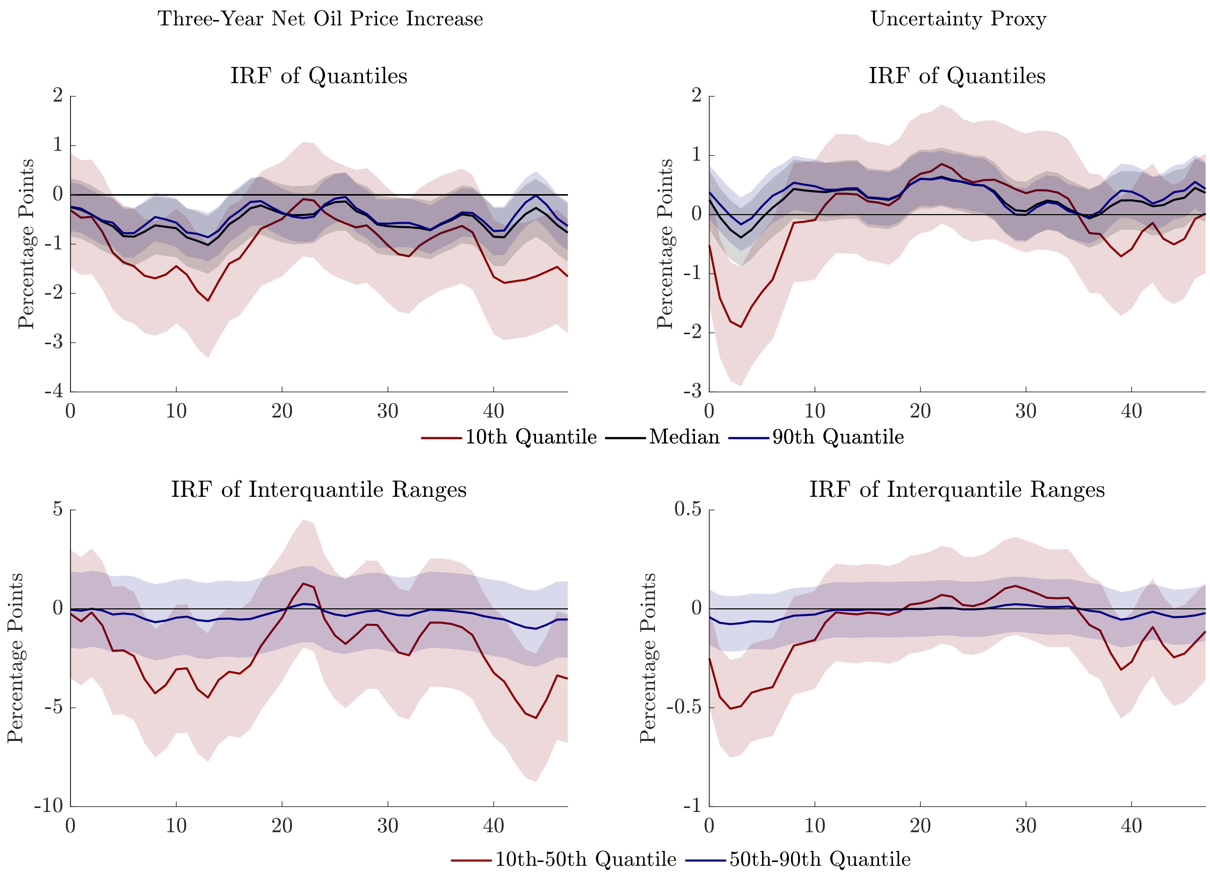

Figure E-6: Impulse Responses of Quantiles of Average GDP Growth over the Next Year to *Contractionary* Shocks. Specification using Monthly GDP Instead of Industrial Production as Dependent Variable.

Note: Red is response of the 10th quantile - 50th quantile, blue is response of the 50th-90th quantile. Confidence bands correspond to median response, 68% significance level, based on bootstrapped standard errors. The x-axis gives the horizon of the impulse response, in months. The response on the y-axis is measured in percentage points.

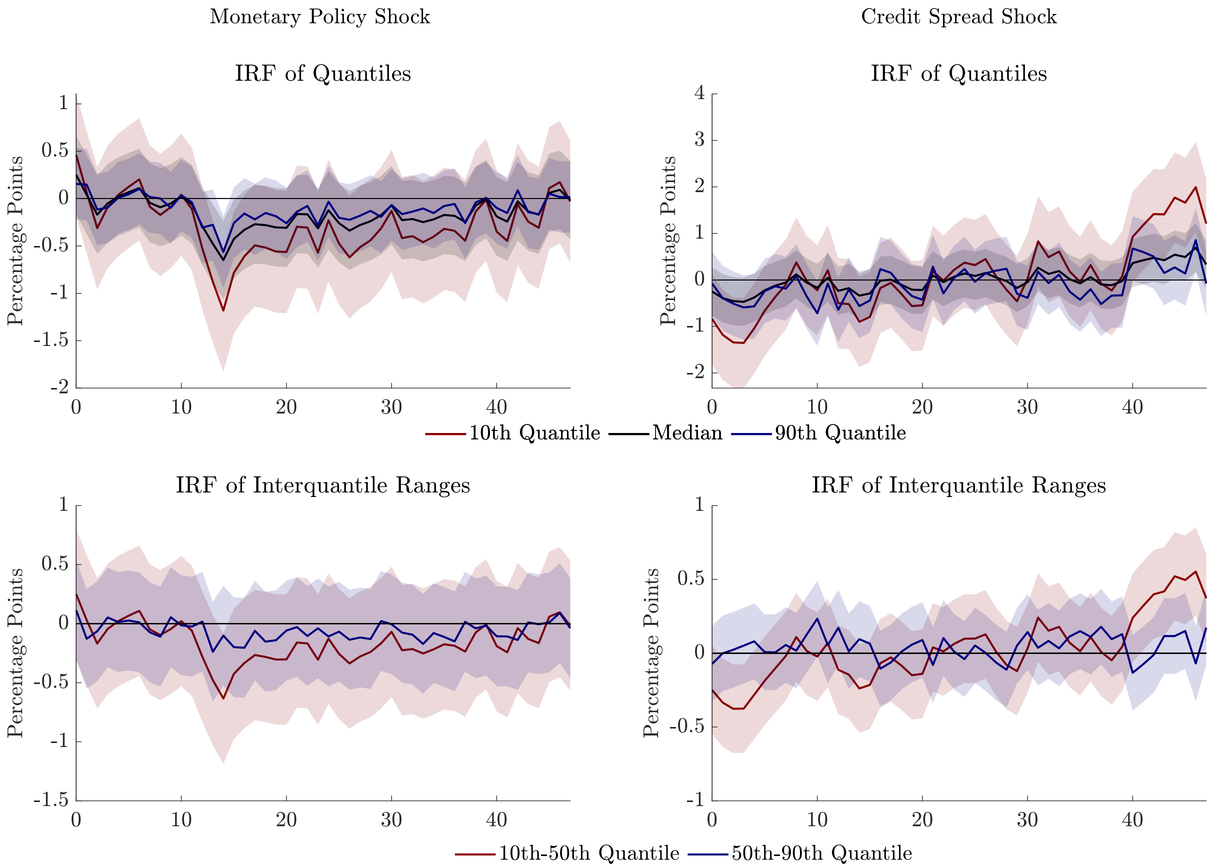

Figure E-7: Impulse Responses of Quantiles of Average Industrial Production Growth over the Next Year to *Contractionary* Shocks. Sample Stopping Before Great Recession.

Note: Red is response of the 10th quantile - 50th quantile, blue is response of the 50th-90th quantile. Confidence bands correspond to median response, 68% significance level, based on bootstrapped standard errors. The x-axis gives the horizon of the impulse response, in months. The response on the y-axis is measured in percentage points.

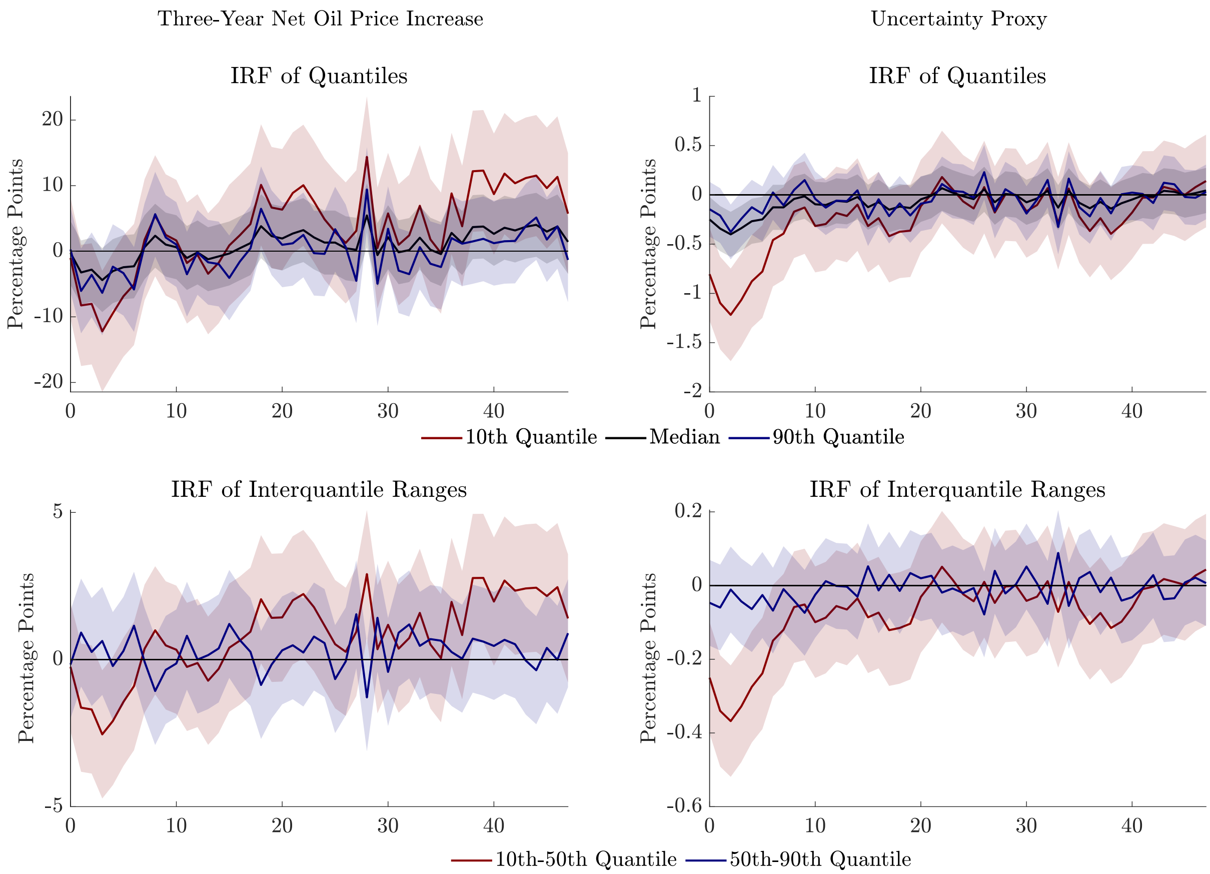

Figure E-8: Impulse Responses of Quantiles of Average Industrial Production Growth over the Next Year to *Contractionary* Shocks. Sample Stopping Before Great Recession.

Note: Red is response of the 10th quantile - 50th quantile, blue is response of the 50th-90th quantile. Confidence bands correspond to median response, 68% significance level, based on bootstrapped standard errors. The x-axis gives the horizon of the impulse response, in months. The response on the y-axis is measured in percentage points.

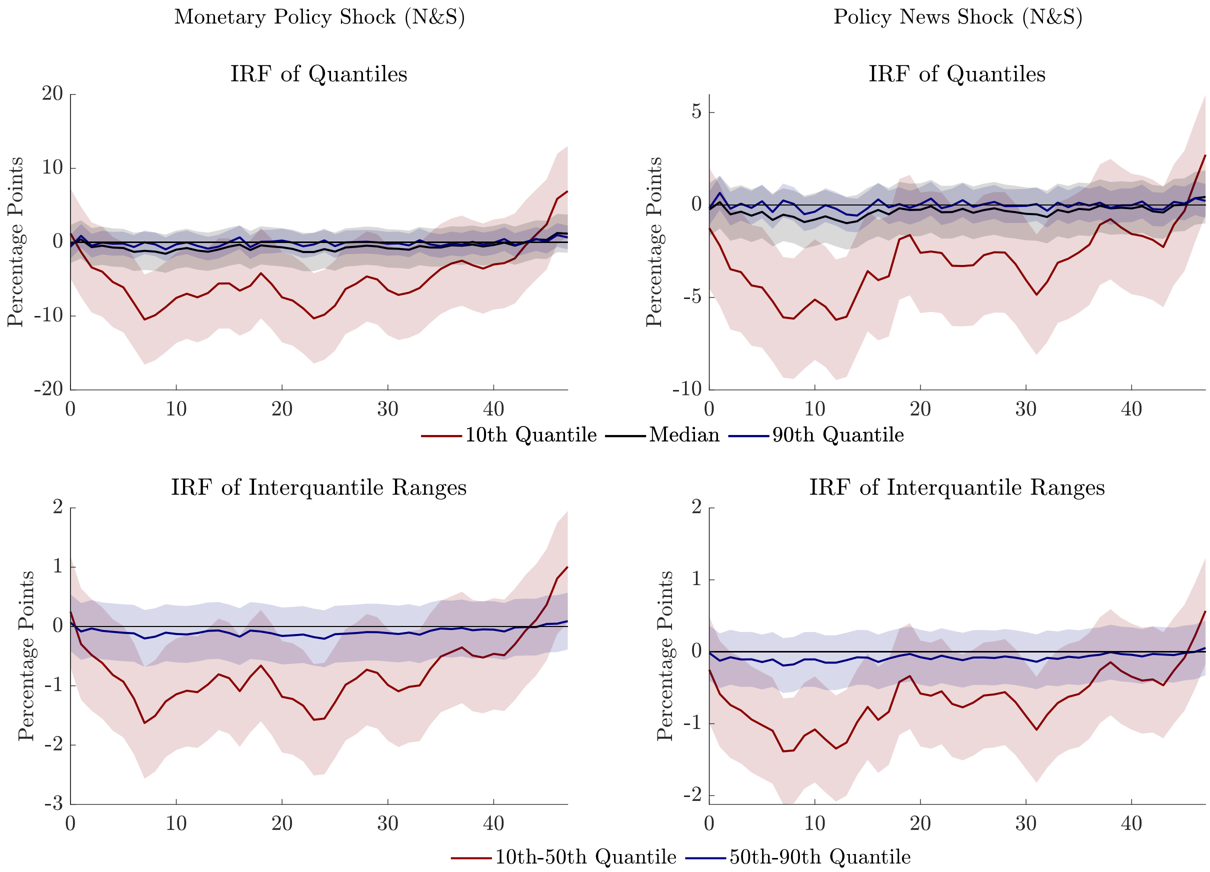

Figure E-9: Impulse Responses of Quantiles of Average Industrial Production Growth over the Next Year to *Contractionary* Shocks. Local Projection Includes Control Variables.

Note: Red is response of the 10th quantile, black is the median response, blue is response of the 90th quantile. Confidence bands correspond to median response, 68% significance level, based on bootstrapped standard errors. The x-axis gives the horizon of the impulse response, in months. The response on the y-axis is measured in percentage points. The monetary shocks are the FFR shock and the policy news shock from Nakamura and Steinsson (2018) (1995 to 2014 sample). Local projection controls for the lagged values of: the shock itself, FFR, CPI inflation, commodity inflation, industrial production growth.

F Inspecting the Relevance of Industrial Production

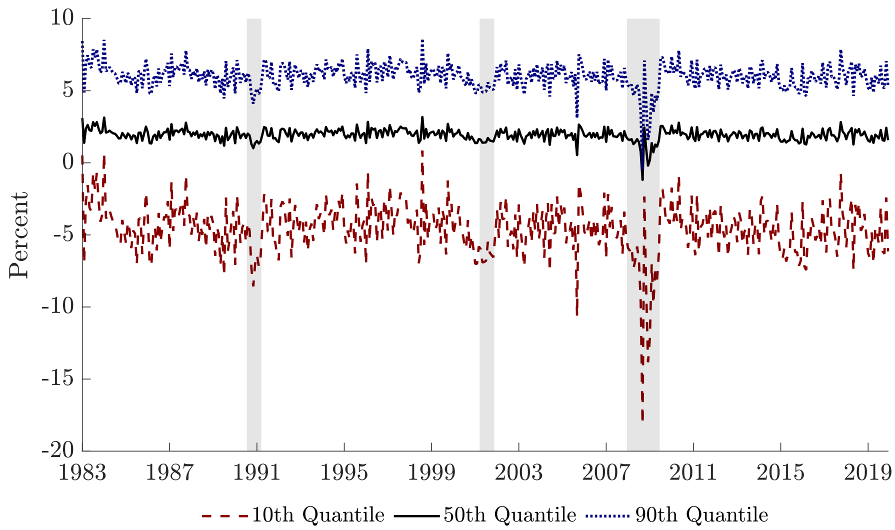

Note: Red is the 10th quantile, black is the median, blue is the 90th quantile. Grey-shaded bars indicate NBER-dated recessions.

Figure F-1: Quantiles of Average Industrial Production Growth over the Next Year Constructed with the Coefficients on NFCI Set to Zero in the QR (3.1).

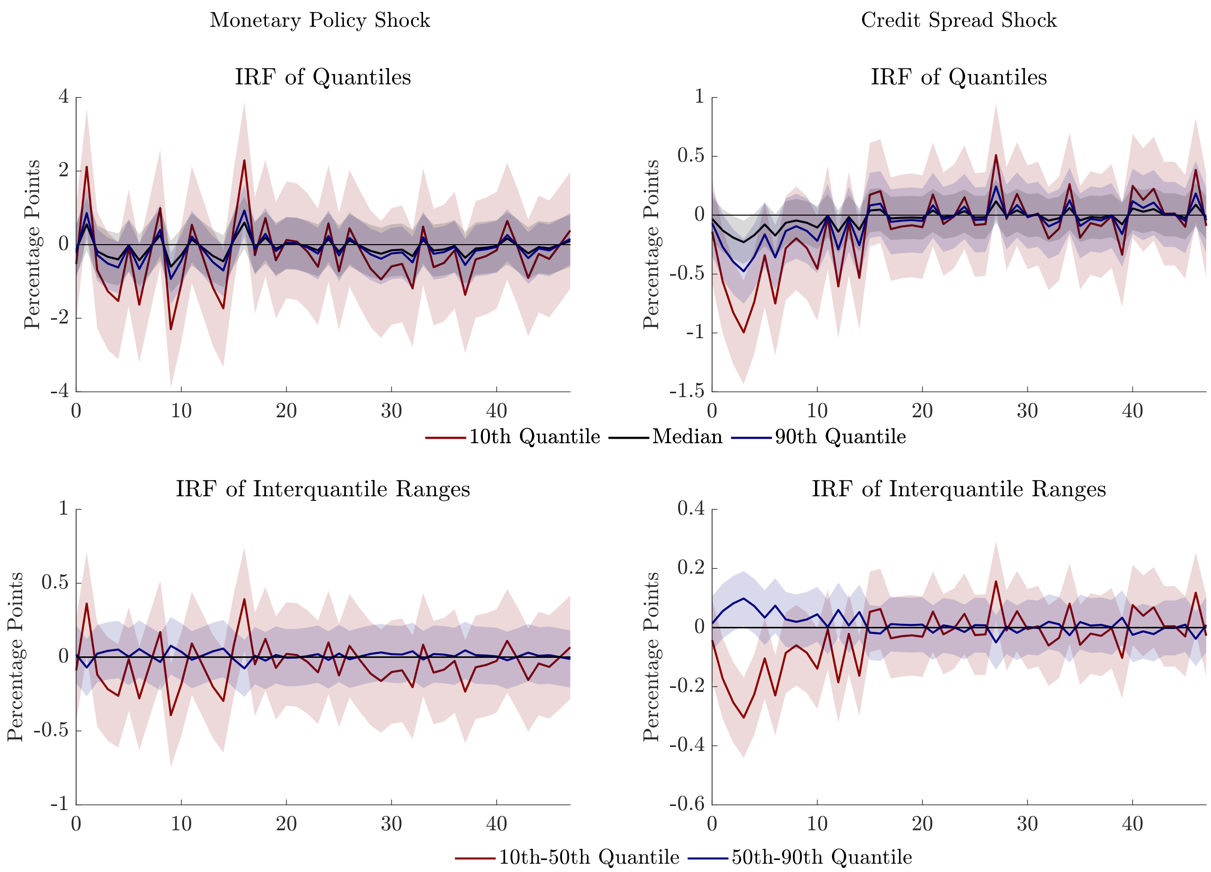

Figure F-2: Impulse Responses of Quantiles of Average Industrial Production Growth over the Next Year to *Contractionary* Shocks. The Quantiles are Constructed with Coefficients on NFCI Set to Zero in the QR (3.1).

Note: Red is response of the 10th quantile, black is the median response, blue is response of the 90th quantile. Confidence bands correspond to median response, 68% significance level, based on bootstrapped standard errors. The x-axis gives the horizon of the impulse response, in months. The response on the y-axis is measured in percentage points.

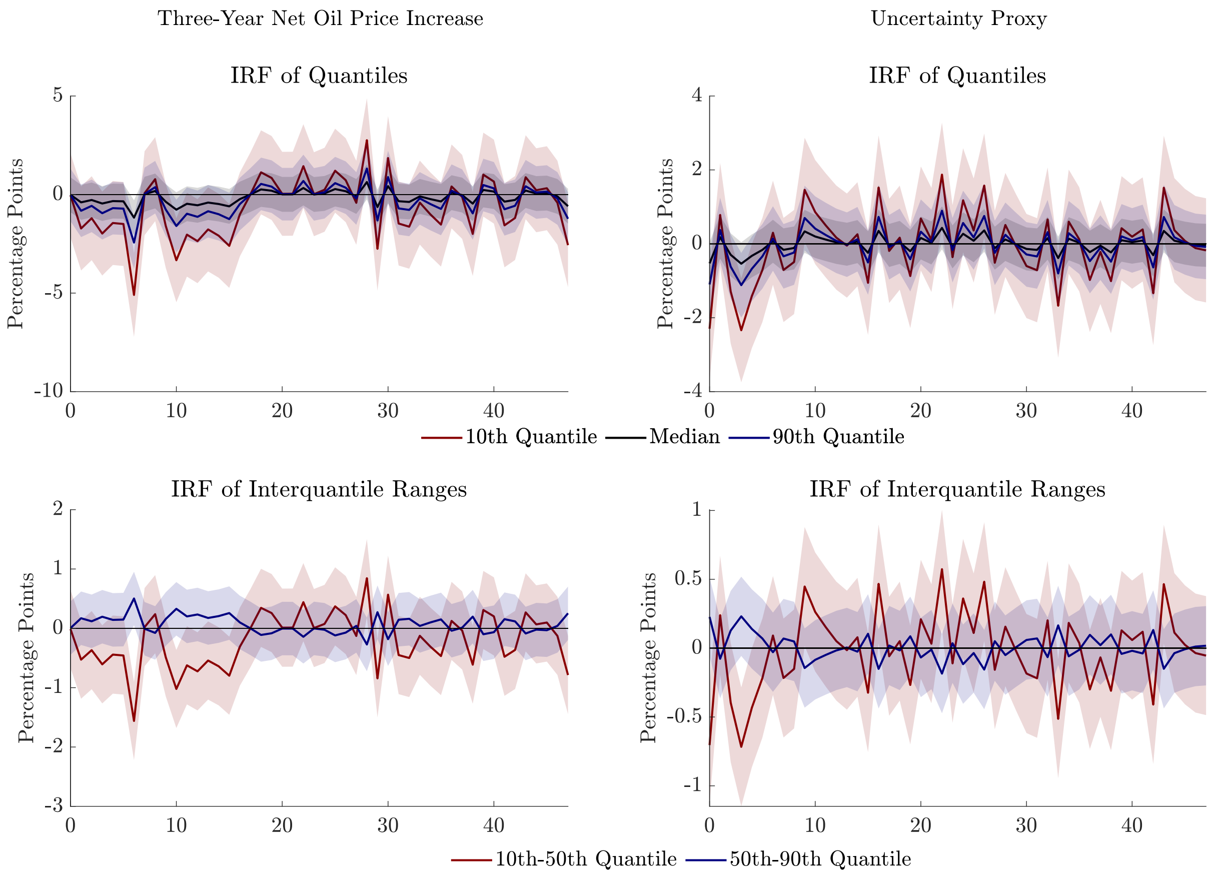

Figure F-3: Impulse Responses of Quantiles of Average Industrial Production Growth over the Next Year to *Contractionary* Shocks. The Quantiles are Constructed with Coefficients on NFCI Set to Zero in the QR (3.1).

Note: Red is response of the 10th quantile, black is the median response, blue is response of the 90th quantile. Confidence bands correspond to median response, 68% significance level, based on bootstrapped standard errors. The x-axis gives the horizon of the impulse response, in months. The response on the y-axis is measured in percentage points.

G Details on Threshold VAR Model

We provide details on the parameter values of the models presented in Subsection 5.1.

The parameters f^* and m^* are chosen such that, on average, the constraint binds in 10% of the sample (on average, across simulations), which is about the percentage of NBER-dated recessions over our sample. $\beta_1 = -0.5$ and $\beta_2 = 0.5$. Negative values for β_1 mean that an increase in f_t is associated with a tightening in financial conditions, which depresses growth. Conversely, positive values for β_2 mean that an increase in m_t is associated with an improvement in macroeconomic activity, which fosters growth.

We assume $\beta_0 = 1$, $\alpha_1 = \gamma_1 = 0.7$ for equal persistence of f_t and m_t, and $\alpha_2 = \gamma_2 = -0.15$ as the financial and macroeconomic factor are negatively related, $\alpha_3 = 1$ and $\gamma_3 = -1$ as a positive (contractionary) shock increases the financial factor (tightens financial conditions) and decreases the macroeconomic factor (weakens economic activity). Further σ_y is set to 0.1.

As to the switching parameters, in model I we assume the following:

$$\alpha_3(f_t, m_t) = \begin{cases} 5, & \text{if } f_t > f^* \ \& \ m_t < m^* \\ 1, & \text{normal state} \end{cases}, \quad \gamma_3(f_t, m_t) = \begin{cases} -5, & \text{if } f_t > f^* \ \& \ m_t < m^* \\ -1, & \text{normal state} \end{cases}$$

In the symmetric model α_3 and γ_3 take on the values of the normal state.

H Showcasing Properties of Our Procedure

Conditioning Variables We showcase how our approach can be informative about which conditioning variable shapes the asymmetry observed in the IRFs. To do this, we consider three models and inspect the IRFs of their conditional growth quantiles.

We start with model III. This is a model where macroeconomic conditions m_t are behind the asymmetry in the IRFs. The top panel of Figure H-1 shows the IRFs of the future real activity growth quantiles that condition on both financial and macro conditions in the first quantile regression (QR) step of our procedure. Not surprisingly the IRFs of the various quantiles respond asymmetrically, similarly to what we documented in Section 5.1. The bottom panel shows the IRFs of the quantiles obtained by setting to zero the coefficient on macro conditions (left) and on financial conditions (right). This is equivalent to what we did in Section 4.2 of the main text. When the partial effect of macro conditions is turned off, our procedure correctly detects that there is no asymmetry in the IRFs of the conditional growth quantiles. Likewise, when turning off the financial channel, our procedure correctly detects that there still is an asymmetry in the IRFs.

Next, we consider model II. This is a model where both financial and macroeconomic conditions are behind the asymmetry in the IRFs. As shown in Figure H-2, our procedure correctly detects that even when considering either the financial or macro channel only, the IRFs of the growth quantiles still exhibit asymmetry.

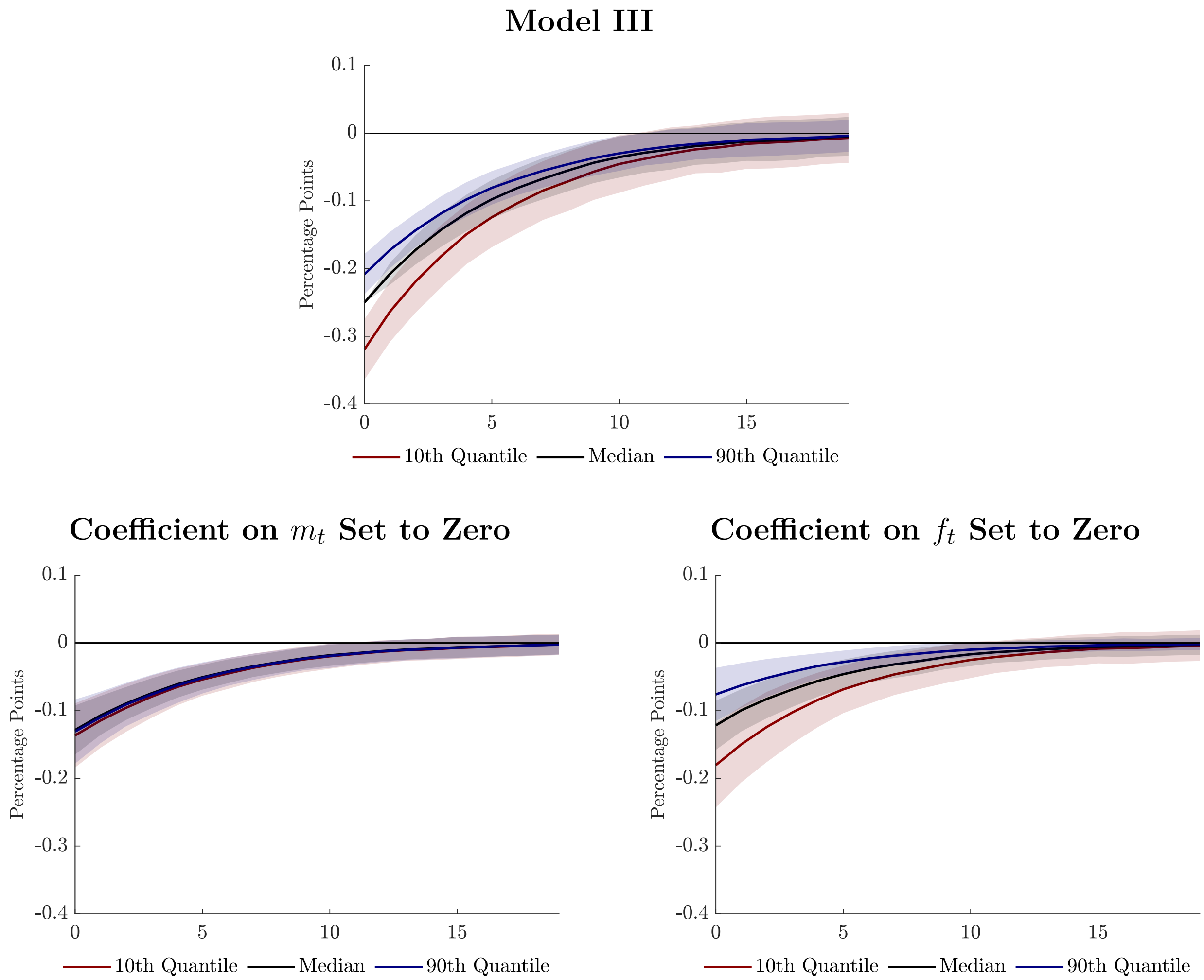

Figure H-1: IRFs of Simulated Future Real Activity Growth Quantiles from Threshold VAR. Model III IRF Decomposition.

Note: IRFs of quantiles that condition on both financial and macro conditions (top panel), IRFs of quantiles that only condition on financial (bottom left panel) and IRFs of quantiles that only condition on macro (bottom right panel). Straight lines are medians across simulations. Shaded areas are 68% confidence bands.

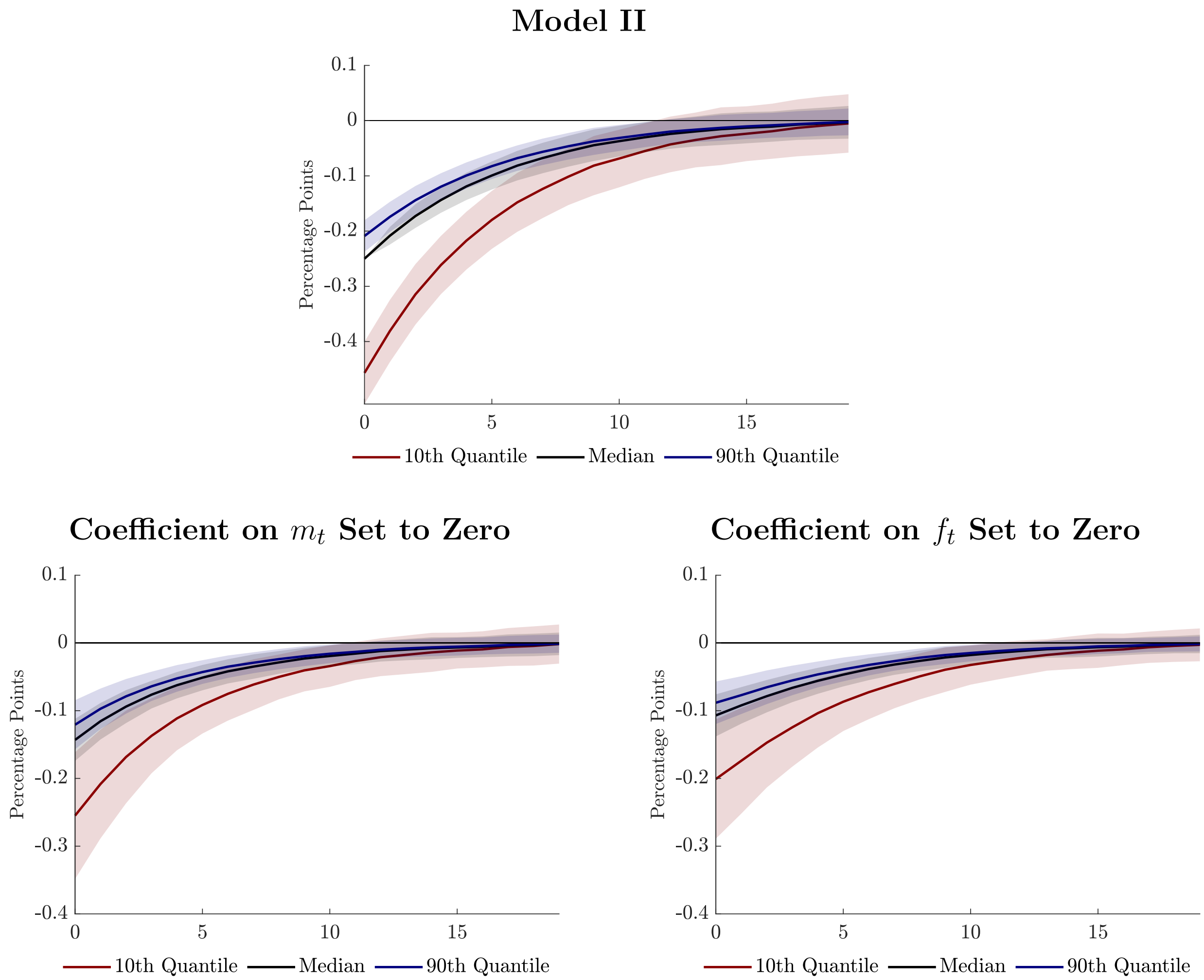

Figure H-2: IRFs of Simulated Future Real Activity Growth Quantiles from Threshold VAR. Model II IRF Decomposition.

Note: IRFs of quantiles that condition on both financial and macro conditions (top panel), IRFs of quantiles that only condition on financial (bottom left panel) and IRFs of quantiles that only condition on macro (bottom right panel). Straight lines are medians across simulations. Shaded areas are 68% confidence bands.

Finally, we consider a modified version of model II (see below). This is a model where macroeconomic conditions drive the asymmetric effect of shocks on real activity growth. As shown in Figure H-3, also in this case our procedure detects that the asymmetry is mainly coming from macroeconomic conditions. The procedure also correctly detects a small (although not statistically significant) asymmetry when only financial conditions are active, which is due to their feedback to macroeconomic conditions (specifically, $\gamma_3 = -0.15$).

Modified Model II *Shock affects f_t and m_t linearly, but their effect on y_t is larger when macroeconomic conditions are bad.*

$$y_t = \beta_0 + \beta_1 f_t + \beta_2(m_t) m_t + e_t^y \tag{H-1}$$

$$f_t = \alpha_1 f_{t-1} + \alpha_2 m_t + \alpha_3 shock_t + e_t^f \tag{H-2}$$

$$m_t = \gamma_1 m_{t-1} + \gamma_2 f_{t-1} + \gamma_3 shock_t + e_t^m \tag{H-3}$$

$$\beta_2(m_t) = \begin{cases} 2.5 \quad \text{if } m_t < m^*; \qquad 0.5 \quad \text{in normal state} \end{cases},$$

where $m^* = -3.2$ so as to maintain about 10% of bad periods in simulation.

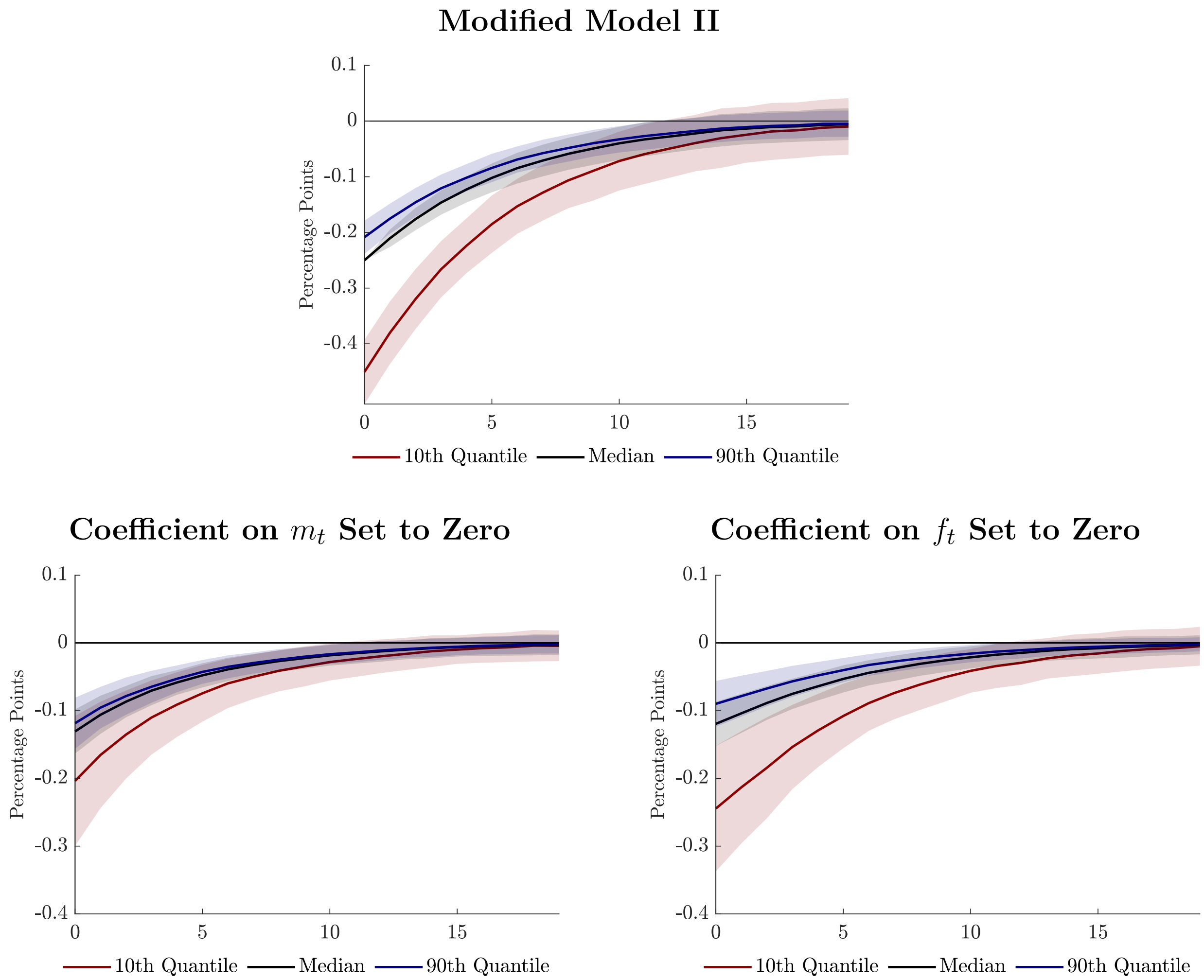

Figure H-3: IRFs of Simulated Future Real Activity Growth Quantiles from Threshold VAR. Modified Model II IRF Decomposition.

Note: IRFs of quantiles that condition on both financial and macro conditions (top panel), IRFs of quantiles that only condition on financial (bottom left panel) and IRFs of quantiles that only condition on macro (bottom right panel). Straight lines are medians across simulations. Shaded areas are 68% confidence bands.

Common Propagation Mechanism We next show that our procedure can be informative on whether shocks share a common propagation mechanism (CPM henceforth). In particular, we show in a modified version of Model I (see below) that when different shocks have a CPM, then their IRFs exhibit a similar pattern when conditioning on the variables governing the CPM. This is illustrated in Figure H-4, which reports the IRFs to the two shocks with asymmetric effects in the modified model I (that is, e_t and $shock_t$), for the baseline case of state-dependent effects (left column) as well as for the linear case where all asymmetries are shut down in the data-generating process (right column). Both shocks exhibit similar IRF patterns in both scenarios, thus confirming that our procedure can be informative about whether a common propagation mechanism underlies the way that shocks affect growth quantiles.

Modified Model I *The two shocks ($shock_t$ and e_t) both have a nonlinear effect on the growth outlook through a common state-dependence/propagation governed by f_t and m_t.*

$$y_t = \beta_0 + \beta_1 f_t + \beta_2 m_t + \sigma_y e_t^y \tag{H-4}$$

$$f_t = \alpha_1 f_{t-1} + \alpha_2 m_t + \alpha_3(f_{t-1}, m_{t-1}) shock_t + \alpha_4(f_{t-1}, m_{t-1}) e_t \tag{H-5}$$

$$m_t = \gamma_1 m_{t-1} + \gamma_2 f_{t-1} + \gamma_3(f_{t-1}, m_{t-1}) shock_t + \gamma_4(f_{t-1}, m_{t-1}) e_t \tag{H-6}$$

where all parameters common to model I take on the same values, and where

$$\alpha_4(f_t, m_t) = \begin{cases} 3, & \text{if } f_t > f^* \ \& \ m_t < m^* \\ 0.5, & \text{normal state} \end{cases}, \quad \gamma_4(f_t, m_t) = \begin{cases} -3, & \text{if } f_t > f^* \ \& \ m_t < m^* \\ -0.5, & \text{normal state} \end{cases}$$

with $f^* = 2.25$ and $m^* = -2.25$ and where in the linear case $\alpha_3 = \alpha_4 = 1$ and $\gamma 3 = \gamma 4 = -1$.

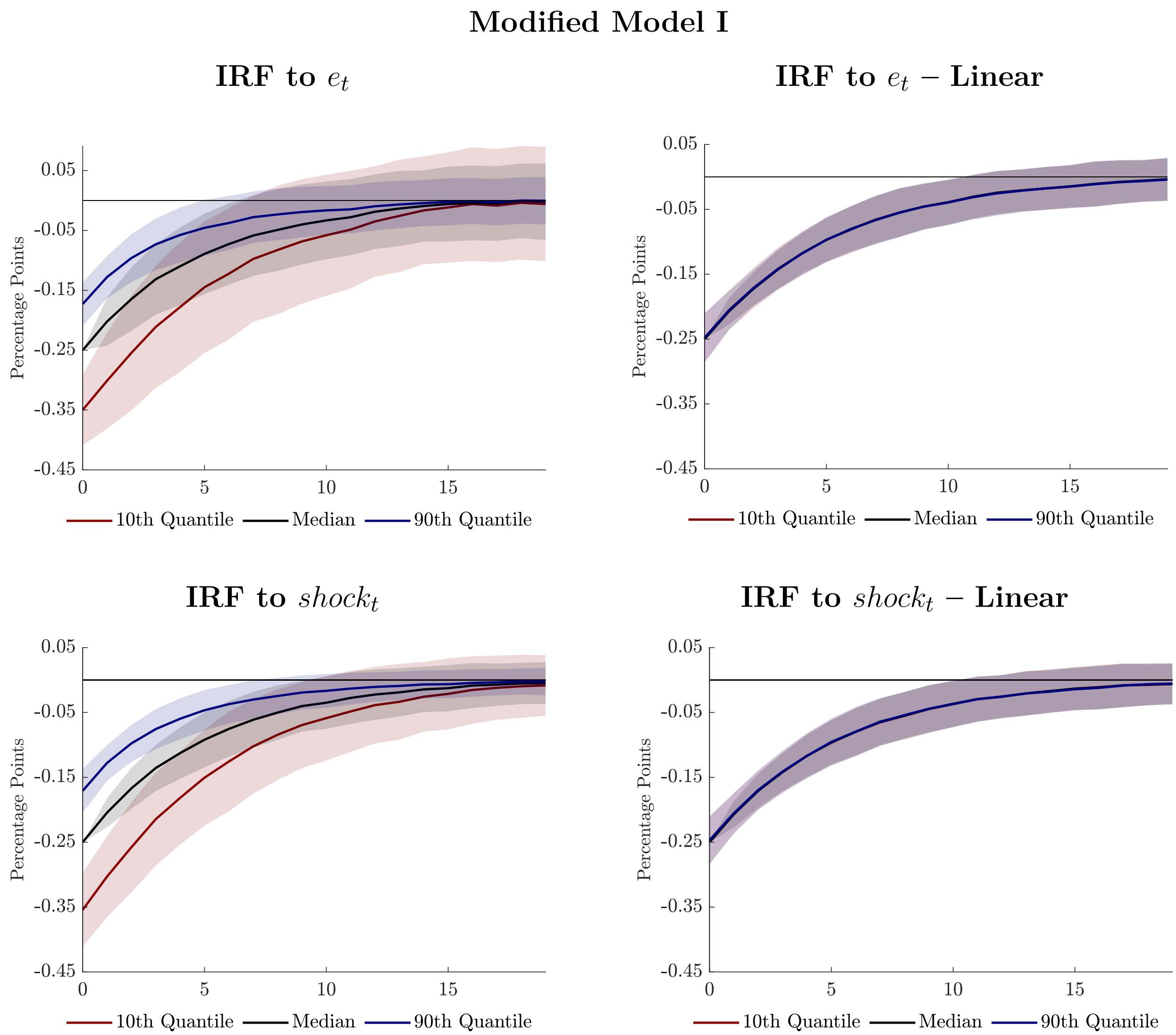

Figure H-4: IRFs of Simulated Future Real Activity Growth Quantiles from Threshold VAR. Modified Model I.

Note: Straight lines are medians across simulations. Shaded areas are 68% confidence bands.

H.1 Additional Threshold VAR Models

Figure H-5 displays the IRFs for a variant of the threshold VAR Model II with non-constant variance discussed in Section 5.1.

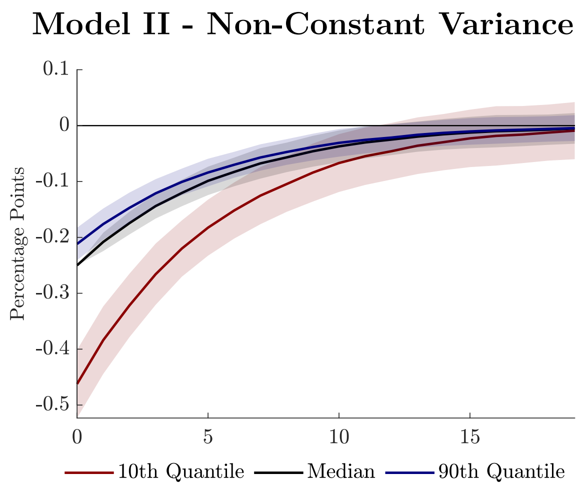

Figure H-5: IRFs of Simulated Future Real Activity Growth Quantiles from Threshold VAR. Model II with switching variance.

Note: Straight lines are medians across simulations. Shaded areas are 68% confidence bands.

I Details on the Gertler *et al.* (2019) Model

Model Solution The model is highly non-linear, and the non-linear effects of structural shocks to the real economy depend on financial conditions. To allow for these non-linear transition dynamics, the model is solved non-linearly using the collocation method with policy functions solved by time iteration. We follow the original paper in focusing on a capital quality shock as a representative structural shock. However, other shocks would give rise to qualitatively very similar results because the mechanism creating asymmetry is not specifically tied to one structural shock.

Parameterization We simulate the model using the original calibration of the deep parameters and of the capital quality shock process (the only fundamental shock in the model). In order to generate rare financial crisis, we calibrate the process for the sunspot shock such that a bank run equilibrium arises after a big negative shock (above two standard deviations).[25]

Simulation We simulate this model 1000 times for 408 periods (the number of periods between January 1986 and December 2019) and store the level of GDP, the credit spread, and the capital quality shock. In our analysis, we treat the credit spread as the equivalent of the financial factor though results are robust to the use of alternative measures of financial conditions in the model. The simulated data shown in the top panel of Figure I-1 indicate that also in this model there is a non-linear relationship between growth and financial conditions. Indeed, large credit spreads are associated with extremely negative growth realizations.

[25] Our calibration intends to make the bank run event (see Figure 2 of the original paper) re-occurring in the simulated sample. In their event study, the authors feed in two consecutive negative capital quality shocks of roughly one standard deviation to push the economy to the edge of the bank-run regime. A third shock, together with a sun-spot shock, then produce the bank run event. We deviate slightly from their event study by having sun-spot shocks occurring concurrently with a negative two standard deviations capital quality shocks to ensure the probability of a bank run of 2.5% across simulated samples.

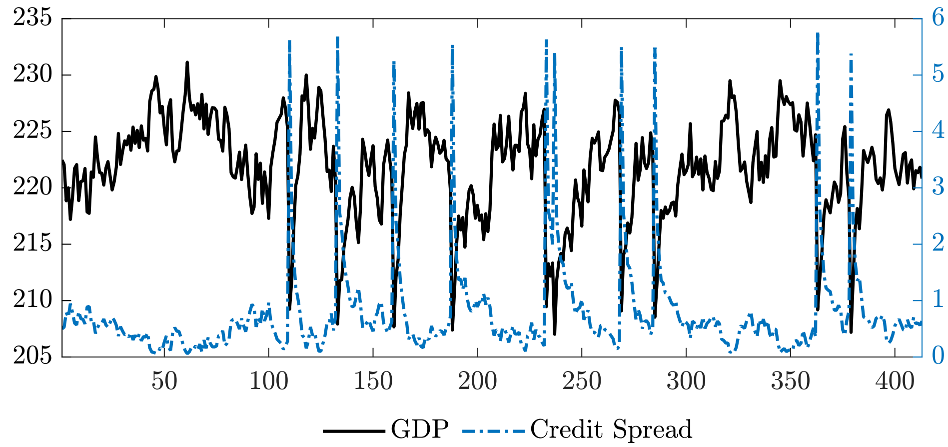

Note: Example from one simulation. GDP (left axis) and Credit Spread (right axis).

Figure I-1: Simulated Data from Gertler, Kiyotaki and Prestipino (2019) Model.

Quantile Regression We focus on current GDP (in deviations from its steady state) as the shocks are transitory and only create a sharp but short-lived recession. Further, we only consider the credit spread as conditioning variable since the non-linearity in the model is mainly coming from financial conditions. As shown in Table I-1, the quantile regression picks up the nonlinear relationship between financial conditions and economic growth, suggesting that financial conditions have a more negative effect on the left tail than on the median.

Table I-1: Quantile Regression Coefficients Estimated on Simulated Data from Gertler, Kiyotaki and Prestipino (2019) Model.

	10th Quantile	Median	90th Quantile
Credit Spread	-10.8	-7.5	-3.7

* Note: Average Across Simulations.

Thus, the left tail of the distribution falls substantially during times of extreme financial distress, characterizing a vulnerable growth outlook.

J Comparison with Linnemann and Winkler (2016)

We now compare our approach in more detail with the approach in Linnemann and Winkler (2016). Let us consider a linear and Gaussian environment where a vector x_t follows a VAR of order 1:

$$x_t = Ax_t + B\varepsilon_t \tag{J-1}$$

with $\varepsilon_t \sim_{iid} N(0, I)$ being a K-dimensional vector of structural shocks. This environment makes our approach substantially less interesting because it does not feature non-linearity. However, it allows us to clarify important distinctions between the two approaches. We can exploit the fact that the median of any Gaussian distribution (which is going to be the quantile we focus on in this example) is equal to its mean. Suppose that we are interested in estimating the effects of the first element of ε_t, which we call ε_t^1, on a scalar variable

$$y_t = cx_t + w_t, \tag{J-2}$$

where c is a row vector and $w_t \sim_{iid} N(0, \Sigma^w)$.[26] Therefore, the "one-step" approach of Linnemann and Winkler (2016) estimates quantiles of the distribution

$$p(y_t | x_{t-1}, \varepsilon_t^1). \tag{J-3}$$

The approach we use first estimates the quantiles of the distribution

$$p(y_t | x_t) \tag{J-4}$$

and then estimates the effects of shocks on those quantiles. In the linear Gaussian case

$$p(y_t | x_{t-1}, \varepsilon_t^1) = N(c(Ax_{t-1} + B^1 \varepsilon_t^1), \Sigma^{\text{one-step}}) \tag{J-5}$$

where a superscript 1 on the matrix B denotes the first column of that matrix. $\Sigma^{\text{one-step}}$ summarizes the effects of shocks w_t and all elements of ε_t except the first one on y_t. One can show that $\Sigma^{\text{one-step}} = \Sigma^w + c\overline{B}(c\overline{B})'$, where $\overline{B}$ is equal to B except for the first column, which is set to 0. The effect of ε_t^1 on the median of this conditional distribution is cB^1.

[26] We focus on the impact effect here for simplicity.

Our approach first estimates the density and then estimates the effects of shocks on those quantiles. In the linear Gaussian case

$$p(y_t|x_t) = N(cx_t, \Sigma^w). \tag{J-6}$$

Plugging in the law of motion of x_t, we can see that

$$p(y_t|x_t) = N(c(Ax_{t-1} + B\varepsilon_t), \Sigma^w). \tag{J-7}$$

The effect of ε^1 on the median of the distribution used in the two-stage approach is then also cB^1. This is the effect that we uncover with the second stage Local Projection in our approach. With the "two-step" approach, we identify c in the first stage (the quantile regression) and B in the second, local projection, stage. Note that then, by setting elements of c to 0, we can assess in the "two-step" approach how shocks are transmitted to the variable of interest y_t via specific elements of x_t, something we cannot do in the "one-step" approach. In empirical applications, we can implement this by constructing counterfactual quantiles using the results from our first stage quantile regressions, as done in the main text.

We have thus shown that in this example both approaches share the same point estimate. Nonlinearities and non-Gaussianity can break this equivalence.

Note that conditioning on x_t in the first step approach would lead to finding no effect of ε_t^1 because once one conditions on x_t, there is no *additional* effect of the shock on y_t.

This example also helps to clarify that both approaches will lead to different measures of uncertainty. This can be seen by comparing the volatility for the density in the "one-step approach" ($\Sigma^{\text{one-step}} = \Sigma^w + c\overline{B}(c\overline{B})'$) with the corresponding volatility for the "two-step" approach (Σ^w). As long as $c\overline{B}(c\overline{B})' > 0$ the "one-step" approach is associated with more uncertainty.

Percentiles other than the Median Unless $\Sigma^{\text{one-step}} = \Sigma^w$ (and thus $c\overline{B}(c\overline{B})' = 0$), the variance of the distribution analyzed in the two-step approach will be smaller. The medians of the two distributions do not coincide (unless $\overline{B}\varepsilon_t = 0$). These differences in first and second moments can lead to any ordering of percentiles across the two distributions. However, in terms of impulse responses, B^1 or changes in ε_t^1 only affect the mean (and not the variance) of either distribution and therefore changes in B^1 or shocks ε_t^1 result in parallel shifts of the distribution and the associated percentiles. This is due to linearity and Gaussianity in this simple example.